Université de Montréal

Photomobility Study of an Azobenzene Derived Molecular Glass

par
Nicole Babich-Morin

Département de chimie
Faculté des arts et des sciences

Mémoire présentée à la Faculté des études supérieures et postdoctorales en vue de l'obtention du grade de maîtrise ès sciences (M.Sc.) en chimie

Août 2019

Université de Montréal
Faculté des études supérieures et postdoctorales

Ce mémoire intitulé

Photomobility Study of an Azobenzene Derived Molecular Glass

Présenté par:
Nicole Babich-Morin

A été évalué par un jury composé des personnes suivantes

Michel Lafleur

Président-rapporteur

Christian Pellerin

Directeur de recherche

Geraldine Bazuin

Membre du jury

Résumé

Les verres moléculaires sont un type de solide amorphe qui ne possèdent pas l'ordre caractéristique d'un cristal. Les verres moléculaires dérivés de l'azobenzène sont le sujet de nombreuses études dû à leur photomobilité, leur capacité à se déplacer sous l'effet de la lumière. Une irradiation à une température inférieure à leur température de transition vitreuse (Tg) produit des cycles d'isomérisation trans-cis-trans à l'échelle moléculaire qui se répercutent en mouvements macroscopiques de la matrice. Ce projet a comme objectif de déterminer si la photomobilité résulte d'une relaxation structurale photoinduite en utilisant le gDR1, un verre moléculaire dérivé du chromophore Disperse Red 1. La spectroscopie UV-visible a été utilisée pour déterminer la fraction d'isomères cis sous irradiation à différentes longueurs d'ondes. Ces longueurs d'ondes ont permis de comparer l'effet d'une irradiation près de l'absorbance maximale de l'un des isomères ou dans les régions peu absorbées par les deux isomères afin de tenir compte de la fraction d'isomère cis et de l'efficacité de l'isomérisation trans-cis-trans. La spectroscopie infrarouge (IR) a ensuite été employée pour mesurer l'impact de l'irradiation sur la température effective locale du groupement azo, de la matrice vitreuse et du groupement espaceur. Malgré une température réelle sous Tg, des augmentations de températures effectives sous irradiation ont été mesurées pour l'azo et l'espaceur. La plus grande augmentation de température effective a été observée pour le groupement azo aux longueurs d'onde d'irradiation provoquant des cycles d'isomérisation efficaces. L'ellipsométrie a permis de mesurer l'expansion photoinduite des films. Les cinétiques de relaxation de la fraction d'isomère cis (UV-vis), des températures effectives (IR) et des changements d'épaisseurs (ellipsométrie) ont ensuite été mesurées pour comparer la relaxation à l'échelle moléculaire et macroscopique du matériau. Finalement, la calorimétrie différentielle à balayage (DSC) a été utilisée pour mesurer des changements enthalpiques du système dus à l'irradiation. Les échantillons ont subi des recuits sous Tg de différentes durées pour leur permettre de tendre vers leur état idéal par une relaxation structurale, ce qui est accompagné par une réduction du volume libre au sein du matériau. L'isomérisation provoquée par l'irradiation a pour effet de produire un excès de volume libre qui est quantifiable en mesurant l'enthalpie associée à la relaxation structurale proche de Tg. Une différence maximale de 1.2 J/g de la relaxation enthalpique en raison d'effets photoinduits a été mesurée, en appui à l'hypothèse voulant que la relaxation structurale contribue

au phénomène de photomobilité. Ce projet contribue ainsi à notre compréhension des phénomènes mécaniques photoinduits sous Tg au sein des matériaux amorphes azos.

Mots-clés: Azobenzène, photomobilité, verre moléculaire, photoisomérisation, relaxation structurale

Abstract

A molecular glass is a type of amorphous solid that lacks the characteristic molecular order found in a crystal. Azobenzene-derived molecular glasses have been widely studied due to their inherent photomobility. Upon irradiation below their bulk glass transition temperature (Tg), they undergo repetitive trans-cis-trans isomerization on the molecular scale that leads to macroscopic motion known as photoinduced mass transport. This project seeks to explore if photomobility is a result of light-stimulated structural relaxation using gDR1, a molecular glass derived from the Disperse Red 1 chromophore. First, UV-visible spectroscopy was used to measure the minimum cis content reached in the photostationnary state under irradiation at various wavelengths. The wavelengths chosen allowed for irradiation near the maximum absorbance of either isomer or in the regions weakly absorbed by both. In doing so, it was possible to consider the wavelength dependence of the material and the effect of the cycling efficiency. Infrared (IR) spectroscopy was then used to probe the effective temperature at the molecular scale of the azo moiety, spacer group and glassy backbone under irradiation. The results showed that despite the bulk temperature of the sample remaining well below Tg, localized effective temperature increases are felt by the molecule upon irradiation. The increase in effective temperature is greatest near the isomerizing azo group and depends on the irradiation wavelength due to the isomerization cycling efficiency. Ellipsometry measurements were then taken to measure photoexpansion of the films. The kinetics of relaxation of the cis content (UV-vis), effective temperature (IR) and thickness (ellipsometry) were compared to evaluate the relaxation process of the material locally and globally. Finally, differential scanning calorimetry was used to measure the enthalpy change in the system resulting from irradiation. Samples were first annealed below Tg for determined times, allowing the material to structurally relax towards its ideal state and thereby reducing its free volume. Upon irradiation, photoinduced cycling generates excess free volume whose impact can be quantified by measuring the enthalpy associated with structural relaxation near Tg. A comparison of the irradiated and non-irradiated samples showed an enthalpy difference of up to 1.2 J/g due to photoinduced effects, supporting the hypothesis that structural relaxation contributes to the photomobility phenomenon. This work thus contributes to understanding photoinduced mechanical changes below Tg in azo-containing amorphous materials.

Key words: Azobenzene, photomobility, molecular glass, photoisomerization, structural relaxation

Acknowledgments

Firstly, I would like to thank Prof. Christian Pellerin for the opportunity to join the Pellerin group and for all of his help and guidance throughout this process. Many thanks also for accommodating my competition and training schedule.

I would like to thank the other students in the Pellerin group, Zeinab Kara Ali, Catherine Lanthier, Geneviève Knapp and Fadwa Ben Amara for their willingness to help me when needed and for their friendship.

I would like to thank Jean-François Myre and Martin Lambert of the department's mechanical shop for fabricating equipment for the project.

Finally, I would like to express my gratitude to my family and friends for their constant support and interest in my endeavors. Specifically, Kristine Kus for always being there for me to talk to, Vincent Lamy for your constant encouragement and lastly, my parents, Sandra Babich and Gary Morin, for the countless hours spent driving me to and from school.

Table of Contents

List of Tables

List of Figures

List of Symbols and Abbreviations

$A_{initial}$	Absorbance prior to irradiation
A_t	Absorbance at given thermal relaxation time
aAB	Aminoazobenzene
ABn	Substituted azobenzene
ATR	Attenuated Total Reflectance
Azo	Azobenzene
DE	Diffraction efficiency
DR1	Disperse Red 1
DSC	Differential Scanning Calorimetry
gDR1	Triazine based molecular glass functionalized with azo chromophore DR1
GFA	Glass forming ability
IR	Infrared
LED	Light-emitting diode
pAB	Protonated azobenzene
pDR1A	Poly(Disperse Red 1 Acrylate)
pDR1M	Poly(Disperse Red 1 Methacrylate)
PMMA	Poly(Methyl Methacrylate)
ppSB	Push-pull pseudostilbene
pSB	Pseudostilbene
SRG	Surface Relief Grating

T_{eff}	Effective temperature
T_f	Fictive temperature
Tg	Glass transition temperature
τ_1	Fast relaxation time constant
τ_2	Slow relaxation time constant
ΔH	Enthalpy

Chapter 1

Introduction

1.1 Introduction to Azobenzenes

1.1.1 Azobenzenes and their Photoisomerization

Azobenzene is a molecule consisting of two phenyl rings joined by an N_2 double bond that is typically found in a thermodynamically stable trans conformation (see Figure 1.1 for structure).

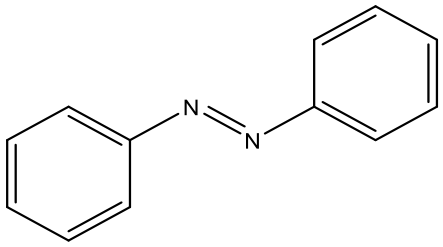

Figure 1.1: Molecular structure of azobenzene in the thermodynamically favoured trans conformation.

Exposure to UV or visible light,[1] electrostatic stimulation[2] or mechanical stress[3] leads it to isomerize to a less stable cis conformation. When left alone, the molecule will isomerize back to its favoured trans conformation. The discovery of azobenzene dates to 1834[4] by Mitscherlich, and while it is most commonly used in commercial dyes, it is the parent compound to a vast collection of derivative molecules whose photochemical properties have been exploited for numerous applications. Reversible changes in their molecular size, shape and dipole moment resulting from UV-Vis light exposure make them useful as small optical and logical devices, small light driven molecular manipulators, actuators and engines, and photochromic molecular switches.[5] They are also employed for imaging plasmonic structures, for tridimensional ordering of microphase separated block copolymers, and for optical fabrication of nano and microstructured surfaces.[6] They are often made as small molecules but they can also be covalently linked to or dispersed in polymers.

Rau divided azobenzene chromophores into three main categories (see Figure 1.2): azobenzenes (ABn) (yellow colour), aminoazobenzenes (aAB) (orange colour) and pseudostilbenes (pSB) (red colour) based on their (n,π*) and (π,π*) transitions energetic ordering.[7]

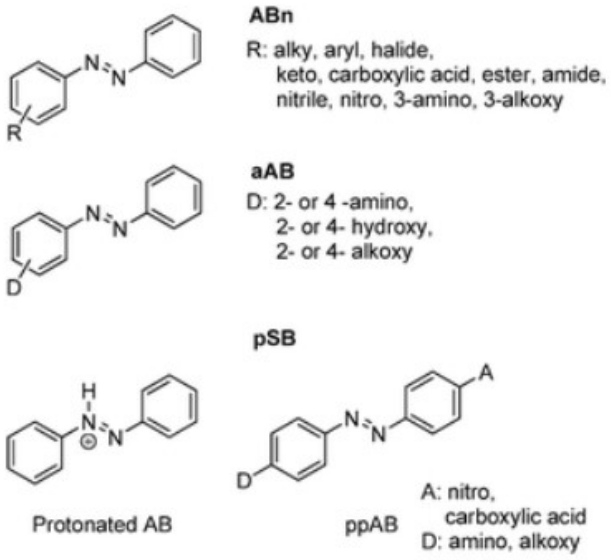

Figure 1.2: The three classes of azobenzenes: substituted azobenzene (ABn), aminoazobenzene (aAB), and pseudostilbene (pSB) with examples of their possible substitutions. Reproduced with permission from ref 3 Copyright (2012) Royal Society of Chemistry.

A low intensity (n,π*) band in the visible region with a high intensity (π,π*) band in the UV region is typical of azobenzenes.[8] Possibilities for their substitution include a halide, an ester, or a carboxylic acid. Aminoazobenzenes are substituted with an electron donating group in the para or ortho positions, which lowers the π* orbital energy and increases the π orbital energy leading to an overlap or near overlap of the (n,π*) and (π,π*) bands in the violet or near UV range.[8] Finally, push-pull pseudostilbenes (pSB) which have an electron donor and electron acceptor group in their 4 and 4′-positions, have a (π,π*) transition with increased charge transfer character resulting in a band red shifted further than the (n,π*) band, with both bands

overlapping or nearly overlapping in the visible region.[3, 8] Protonated azobenzenes also fall into the category of pseudostilbenes.[3]

The ability of azobenzene to isomerize from its trans to cis form under UV light exposure, then thermally relax to its trans form when the light is turned off, was discovered in 1937 by Hartley.[1] This phenomenon is termed photoisomerization, and it is a quick, efficient and reversible reaction between two isomers that have different properties and structures.[9] The distance between the para positions on azobenzene has been shown to decrease from 10.0 to 5.6 Å while the average free volume requirement increases to 0.2 nm^3 in isomerising from its trans to cis form.[10] Hartley discovered that during irradiation the solubility of azobenzene changes.[11] In polar solvents, the cis isomer was more soluble than the trans isomer because of its higher dipole moment.[12] As shown in Figure 1.3, the trans isomer is stable, planar and non-polar, with an absorbance maximum at 330 nm, while the cis isomer is metastable, non-planar and polar, with an absorbance maximum at 350 nm.[9]

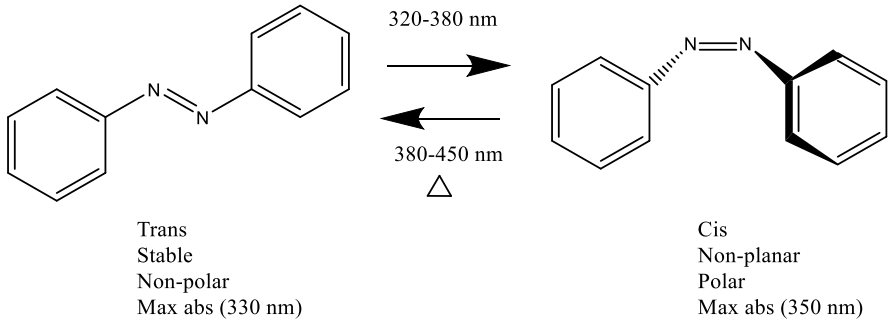

Figure 1.3: The photoisomerization reaction of trans azobenzene into cis azobenzene under UV light irradiation as well as reverse isomerization from the cis to trans isomer occurring by heating or irradiation with visible light.

Four pathways have been suggested for the isomerization of azobenzene: the inversion mechanism, the rotation mechanism, the concerted inversion mechanism, and the inversion-assisted rotation mechanism, as illustrated in Figure 1.4.[3] However, there is still a dispute as to which one is correct.[9] In the inversion mechanism, the N=N-C angle undergoes an in-plane increase, meaning it increases to 180° with the dihedral angle of the C-N=N-C remaining fixed

at 0°.[3, 9, 13] In the rotation mechanism, there is free rotation around the N-N-C bond fixed at 120° by breaking the N=N π bond, allowing the dihedral angle (C-N-N-C) to rotate.[6] The concerted inversion mechanism involves creating a linear transition state by increasing the two N=N-C bond angles to 180°.[3] Finally, with the inversion-assisted rotation mechanism, the N=N-C angle undergoes small changes at the same time that the C-N=N-C dihedral angle undergoes larger changes.[3] All of the mechanisms involve polar transition states with the exception of the concerted inversion mechanism where the transition state has no net dipole moment.[3]

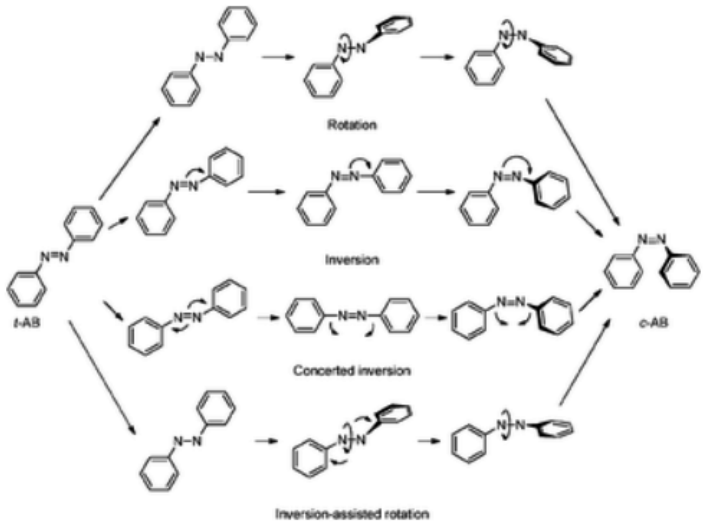

Figure 1.4: Reaction mechanisms for the four proposed isomerization pathways of trans azobenzene into cis azobenzene; rotation, inversion, concerted inversion, and inversion-assisted rotation. Reproduced with permission from ref 3 Copyright (2012) Royal Society of Chemistry.

In addition to thermally relaxing in the dark, the cis isomer can be driven back to the trans isomer with light. Figure 1.5 shows a comparison of the absorption spectra of the trans (π,π*) band and cis (n,π*) band for isomers of the azobenzene type. For example, irradiation with UV light powers the trans-cis isomerization through absorption of the (π,π*) band while irradiation with visible light powers the cis-trans isomerization by absorption of the (n,π*) band.[7]

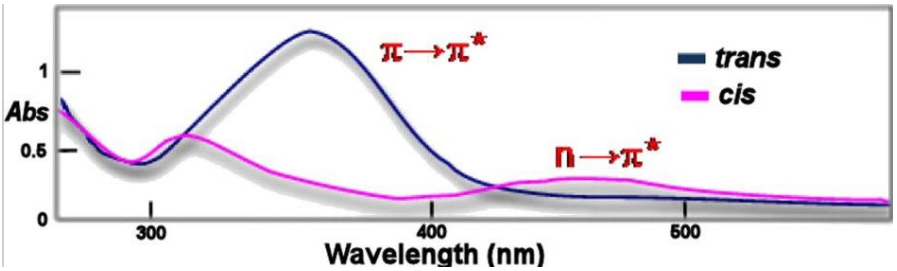

Figure 1.5: Absorption spectra an azobenzene type molecule demonstrating the (π,π*) absorption band of the trans isomer and the (n,π*) absorption band of the cis isomer. Reproduced with permission from ref 7 Copyright (2002) Elsevier.

The thermal relaxation of azobenzene's cis isomer to its thermodynamically stable trans form is slow compared to most of its derivatives, making it an ideal choice for studying the cis isomer.[11] Excluding a few sterically hindered molecules, reversible trans-cis isomerization is possible with all azobenzene derivatives (also called azos), as they generally share a basic geometry that is modified by electronic and steric effects of the derivatives.[11]

ABn type derivatives typically relax faster (minutes or seconds in solution) than unsubstituted azobenzene (days) but have a similar quantum yield of photoisomerization (typically around 0.2 for trans to cis).[3, 8] Their isomerization is accomplished though UV-Vis light exposure and they are usually chosen for applications needing a slower relaxation than pSBs, such as protein probes.[3] For example, they can participate in enzyme inhibition when an azobenzene moiety is inserted inside a DNA sequence.[14] They are also sought after for light-driven molecular machines that require converting electromagnetic radiation into mechanical work[3] such as unidirectional rotors or tweezers where photoinduced changes to an azo moiety causes the movement of a guest molecule that has been non-covalently linked.[15] aABs are most commonly found in industrial dyes,[3] in photoresponsive polymers,[16] and in photoelectric and information storage devices.[17] By slightly raising the electron density in the π* orbital, through substitution with electron donating groups, aABs lower the barrier for thermal isomerization.[3] They relax faster (milliseconds or seconds) and have a higher quantum yield of photoisomerization (up to 0.8) than ABn derivatives.[3] They have been used as laser beam operated molecular machines because when irradiated with plane polarized light, only the aABs

aligned in the direction of polarization will isomerize, allowing photoselective volume contraction that results in a material that bends.[18] In the presence of strong acid, azobenzene can be protonated to give pAB, one type of pSBs, that is highly fluorescent if frozen in a solid matrix, distinguishing it from the other type of pSBs.[3] They form the more stable cis isomers of the pSB type with a half life of the order of minutes.[7] The other type of pSBs, push-pull azobenzenes, thermally relax on the order of milliseconds or seconds.[3] They are typically found in industrial dyes, owing to their intense red colouring[3], as well as in holographic memory storage devices,[19] and surface relief gratings.[20] Push-pull type azobenzenes are discussed in more detail in section 1.1.2.

The rate of thermal relaxation of an azo after isomerization is influenced by several factors in addition to its chemical structure. Studies have been done on the effect of the azo's environment on the yield of isomerization. The absorption band of an azo dye in solution has an intensity, shape and maximum absorption wavelength that depends on the nature of the solvent and on solute-solvent interactions.[21] Figure 1.6 shows the changes in the absorption spectra of a push-pull azo dye, Disperse Red 1 (DR1, structure shown in Figure 1.8), in different solvents.

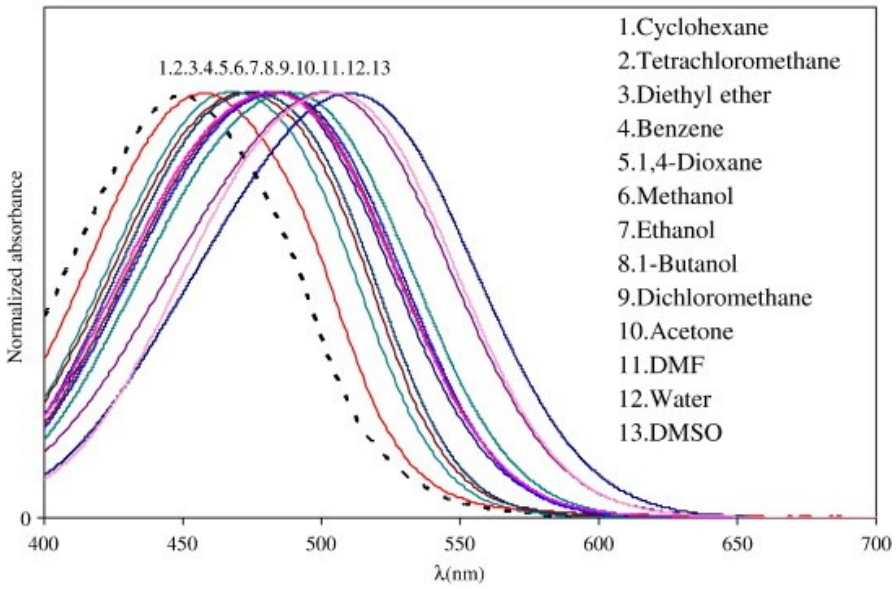

Figure 1.6: Normalized absorbance spectra of the azobenzene dye derivative DR1, of the push-pull type, in varied solvents of different viscosity, acidity and dielectric constant. Reproduced with permission from ref 22 Copyright (2010) Elsevier Inc.

A study about the effect of different solvents on the isomerization process showed that those with a high dielectric constant increase the yield of trans-cis isomerization and decrease the rate of thermal cis-trans isomerization.[7] The rate of isomerization can be increased using acidic solvents while the use of viscous solvents will have no effect on the quantum yield of isomerization.[3] Temperature has a limited influence over the quantum yield of isomerization.[3] Decreasing the temperature results in a small decrease in trans-cis isomerization. However, cis-trans isomerization is not significantly impacted.[7] The photostationary state, the state where photoinduced isomerization is in equilibrium, will therefore have a higher fraction of trans isomers. Temperature independent cis-trans isomerization of azobenzene has been observed at temperatures nearing 4 K and is therefore possible at very cold temperatures and in frozen solvents.[7] Faster cis-trans thermal relaxation rates are observed when the azo's absorption maximum is shifted to higher wavelengths, implying a smaller steady state fraction of the cis isomer under irradiation.[4] An example of an application that is impacted by the lifetime of the cis isomer is the design of red and near-IR photoswitches. These photoswitches require a cis isomer with a long lifetime and, therefore, the energy barrier between cis and trans isomers as well their relative energies will determine if the photoswitch will function.[4] Another application that depends on the cis isomer's lifetime is holographic data storage, where a short lifetime is favourable for orienting the chromophores perpendicular to the axis of the plane polarized light, changing the refractive index of the material, and thereby storing information.[3]

1.1.2 Photoinduced Motion of Azobenzenes

To exploit their photoisomerization, azos have been covalently linked to polymers, small molecules and molecular assemblies, as well as used as films and gels.[7] Typically, amorphous materials, such as polymers and molecular glasses, have very slow cooperative segmental motion below their bulk glass transition temperature (Tg). However, when azobenzene derivatives isomerize quickly from their trans to cis forms repeatedly in the solid state, the motion of azo groups on the molecular scale can induce macroscopic motion well below Tg.[22-23] This feature is called photomobility and is not yet well understood. Free volume, the lifetime of the cis isomer, and the nature of the azo chromophore are fundamental concepts in its study.

Since the mid 1990's, azobenzene derivatives have been used in the formation of surface relief gratings (SRG), whereby a topological relief is made on an azo film from a polarized light interference pattern.[22] This is accomplished by movement on a macroscopic scale, known as photoinduced mass transport,[24] that depends on the photomobility phenomenon. Figure 1.7 illustrates the formation of a surface relief grating using azo-functionalized dendrimers.

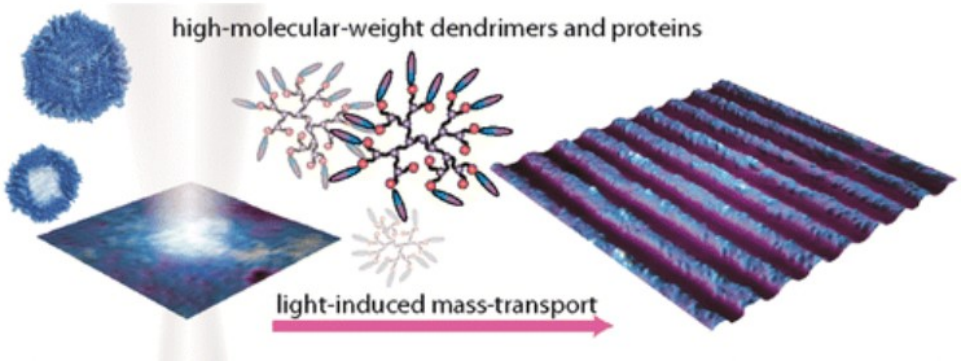

Figure 1.7: Schematic representation of the formation of a surface relief grating by light-induced mass-transport using azo-functionalized triazine dendrimers and proteins of high molecular weight. Reproduced with permission from ref 25 Copyright (2014) American Chemical Society.

The free volume around the molecule plays a role in its ability to undergo photoisomerization. In the case of azos, the volume required for the isomers to move and isomerize is greater than that occupied by stationary trans and cis isomers. It has been determined that azobenzene in solution requires a free volume of 0.12 nm^3 to isomerize by inversion and 0.25 nm^3 to isomerize by rotation.[25] When isomerization occurs in a pocket of a host material with a volume that is smaller than the free volume needed, a local pressure can be generated.[11] It has thus been suggested that photoinduced pressure is a likely mechanism that allows molecular scale isomerization to result in macroscopic motion, and the role of external pressure on the formation of the cis isomer has been studied.[11] The results of this study are discussed in more detail below. The molecular structure of the azo plays a role in photoisomerization. The local mobility of an azo also depends on the strength of its coupling interaction with the host material, for example a polymer, its size, and the free volume available

around it.[26] For instance, bulky substituents on azobenzene can decrease the quantum yield of photoisomerization because they increase the free volume requirement of isomerization.[26]

As mentioned, the chemical nature of the azo chromophore plays an important role in its photoactive properties. Azos with a push-pull character are often chosen when studying photomobility. An example of an azobenzene derivative with push-pull character is Disperse Red 1, or DR1, a polar, nonlinear-optical chromophore (see Figure 1.8 for structure).[27]

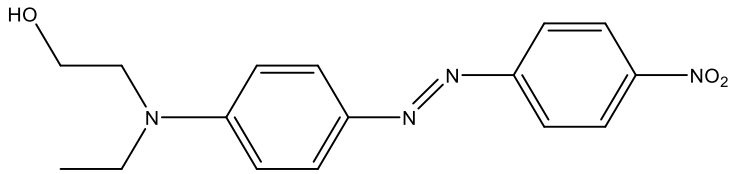

Figure 1.8: Molecular structure of the azobenzene derived push-pull Disperse Red 1 (DR1) chromophore.

Substitution with electron donating and electron withdrawing groups favours photoalignment of chromophores irradiated with polarized light, which is required for SRG formation.[28] The (π,π*) absorption band of DR1 is red shifted into the visible region from the near UV region, as compared to unsubstituted azobenzene, due to the push-pull character creating a strong charge transfer character in the (π,π*) electronic transition, where it overlaps with the (n,π*) transition that is usually weaker.[5] The cis-trans thermal relaxation of DR1 in solution is much faster than that of azobenzene, on the order of milliseconds (depending on the solvent), because the energy barrier between the isomers in the S_0 ground energy state is lowered.[5] This facilitates isomerization and prohibits a large build-up of the cis isomer in the photostationary state.[4] Linearly polarized light will induce an anisotropic orientation of DR1 through trans-cis-trans photoisomerization cycling, which can then be erased with circularly polarized or unpolarized light.[27] The hydroxy group of DR1 can be used as a covalent or non-covalent linker to make other derivatives for various uses.[5] It is often linked to polymers or small molecules to make amorphous materials such as poly(Disperse Red 1 Acrylate) (pDR1A) (see Figure 1.9 for structure). Since the 1990's, pDR1A has been studied for its stability in data

storage, fast switching, photorefractivity and photoorientation, which make it useful in holographic, photonic and optical applications.[11]

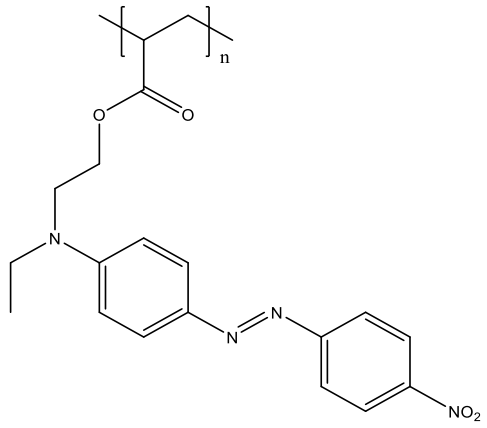

Figure 1.9: Molecular structure of poly(Disperse Red 1 Acrylate) (pDR1A).

The polymer has been used in many experiments to study the effect of the azo group in terms of the free volume involved in photoisomerization. In one study, Barrett and coworkers investigated the effect of external pressure on the formation of the cis isomer of pDR1A with a Tg of 79 °C. As the pressure was increased above ambient pressure, the cis fraction in the photostationary state decreased, which was attributed to the free volume in the film being reduced, allowing fewer chromophores to photoisomerize from the trans to cis form.[11] The cis content as a function of pressure is shown in Figure 1.10. The authors also found that the half-life of cis-trans thermal relaxation increased, indicating that increasing the external pressure on the azo polymer lowers both the yield and the rate of isomerization.[11] In another study on pDR1A (Tg of 95 °C), the same group explored the impact of temperature on the free volume available for photoisomerization. Below a temperature of 50 °C, photoexpansion occurred to "accommodate the free volume requirements of the azo isomerization" and while the polymer network expanded, the chromophores could only move on a small scale in their free volume pockets because the overall polymer network was stationary.[29] When the temperature was above 50 °C, photocontraction occurred as the polymer had a higher mobility, with the expansion counteracted by relaxation in the network, allowing the chromophores to "reorient within the

polymer matrix, aggregate and create a denser contracted state" by light irradiation at temperatures that fall below but close to their Tg.[29]

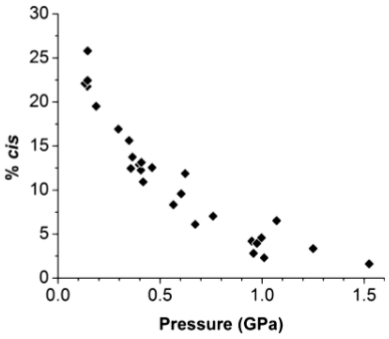

Figure 1.10: Percentage of cis isomers in the photostationary state as a function of the external pressure observed for pDR1A under 532 nm irradiation. Reproduced with permission from ref 11 Copyright (2012) American Chemical Society.

1.1.3 Selected Photoisomerization Studies

In addition to making SRGs, where there is a phase modulation of the polymer surface, it is possible to make volume gratings where there is an intensity modulation of the refractive index or the absorption coefficient.[10] An early study on pDR1A found that it could repeatedly make volume gratings that are written by the interference of circularly or linearly polarized light beams and erased thermally or by short exposure to a single circularly or linearly polarized beam.[10] The laser intensity only influenced the rate of formation since the grating diffraction efficiencies saturated at the same value for all irradiation intensities. A low initial efficiency was reached in a fast process (seconds) that was followed by a slower process (minutes) leading to high efficiency. It was noted that the process was only reversible when the exposure to the writing beam lasted only for a few seconds. The efficiency of the SRGs prepared was impacted by the geometry of the irradiation, the laser irradiance and polarization as deeper gratings were made with circularly polarized light as opposed to linearly polarized light.

A few key factors were identified for the formation of the gratings. Firstly, the process only occurs if the chromophore has azo groups, and secondly, the cis content, which depends

on laser irradiance and temperature, falls between 5 and 10 % for pDR1A, starting from a mostly all trans state prior to exposure. Thirdly, as shown in Figure 1.11, the gratings with the highest efficiency are formed from chromophores needing the largest free volume when comparing polymers of similar Tg and molecular weight.[10]

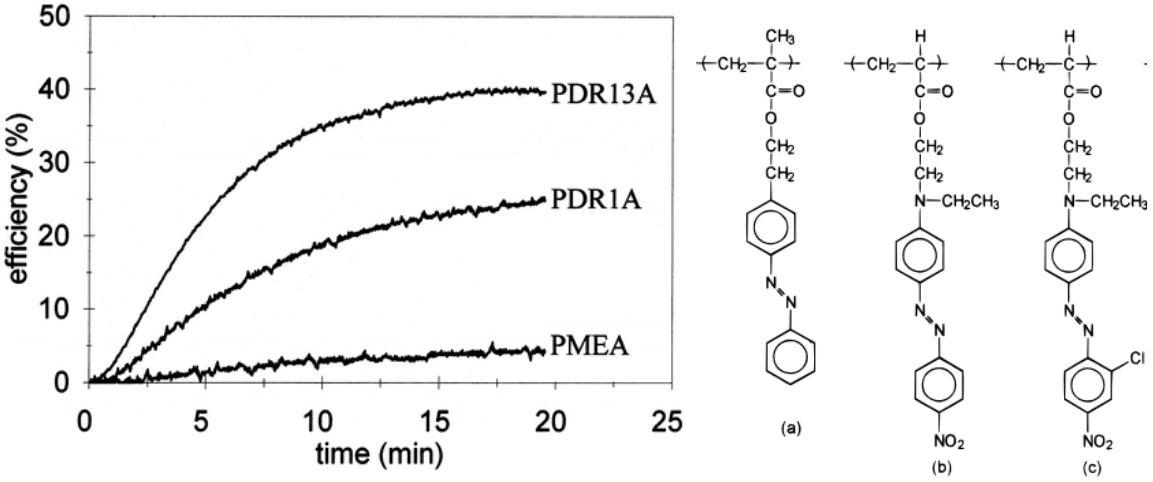

Figure 1.11: Diffraction efficiency vs time for three films (close to 800 nm thick) of polymers of the azobenzene type (a) PMEA, and the push-pull type (b) pDR1A, and (c) pDR13A under irradiation at 488 nm. The polymers are of similar molecular weight and Tg but require different free volume changes for isomerization. Reproduced with permission from ref 10 Copyright (1996) American Chemical Society.

The influence of the chemical nature of the polymer backbone used, substituted with the same selected azo chromophore for photoinduced SRG formation, has also been studied.[30] The authors prepared vinyl, acrylate and methacrylate polymers with a [di(biphenyl-4-yl)amino]azobenzene side chain. The molecular structures of the polymers are given in Figure 1.12. The Tg's of the polymers were higher (120-160 °C) than that of the parent compound consisting only of the side chain molecule (68 °C). After irradiation with 450 nm light, all of the compounds showed similar cis fractions in the photostationary state, which was explained by the azo group's photochromic behaviour being independent of the polymer backbone. The acrylate polymer showed the fastest SRG inscription rate followed by the methacrylate and then the vinyl polymer. The slower SRG inscription with the vinyl polymer was explained by the

azo's lower flexibility as compared to the acrylate and methacrylate polymers that had an ester spacer group between the main chain and chromophore. The methacrylate polymer had the highest diffraction efficiency followed by the acrylate polymer and the vinyl polymer. This was explained by a combination of the effect of higher mobility of the azo groups with the ester spacer and the effect of increasing Tg favouring SRG formation.[30]

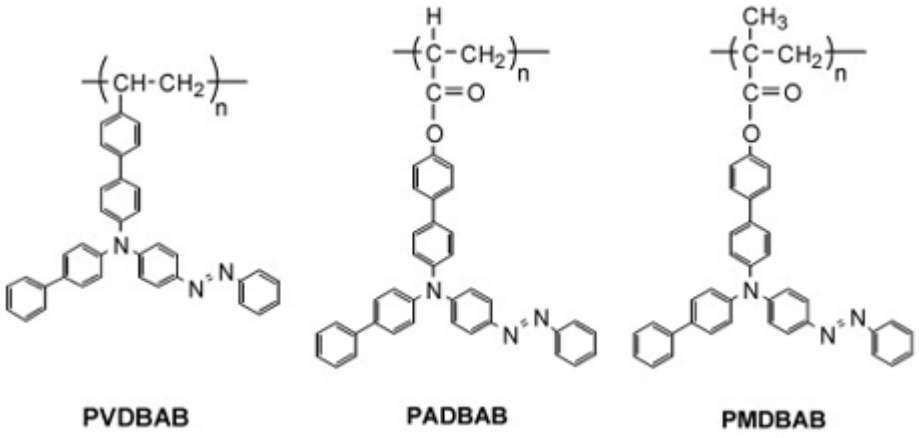

Figure 1.12: Molecular structures of poly(4′-{N-biphenyl-4-yl)-N-[4-(phenylazo)phenyl]amino}biphenyl-4-ylethylene) (PVDBAB), poly(4′-{N-biphenyl-4-yl)-N-[4-(phenylazo)phenyl]amino}biphenyl-4-yl acrylate) (PADBAB), poly(4′-{N-biphenyl-4-yl)-N-[4-(phenylazo)phenyl]amino}biphenyl-4-yl methacrylate) (PMDBAB). Reproduced with permission from ref 30 Copyright (2009) Elsevier Inc.

A more recent study has investigated the relationship between the reorientation probability of azo doped polymers and the wavelength of irradiation.[31] In this work, the reorientation probability was dependent on the wavelength of irradiation in terms of photon energy and the number of reorientation attempts giving the quantum yield of isomerization. The authors concluded that the reorientation of a molecule is influenced by the photon energy it absorbs.[31]

As previously mentioned, holographic data storage is one of the applications of azo polymers. DR1-doped PMMA polymers have been used to make holograms by the interference of two coherent laser beams that are controlled by an incoherent beam.[32] The authors were able to tune the orientation polarizations of the recording beams and the assisting beam to increase or decrease the light diffraction. Holograms made by an intensity modulation were found to be highly dependent on the polarization of the incoherent beam while holograms made by polarization modulation did not depend on the polarization of the incoherent beam. For the intensity modulation holograms, the diffraction efficiency decreased when the assisting beam was parallel to the recording beams, and it increased when the beams were perpendicular.[32] Holographic patterns made with azopolymers also have biological applications as they can serve as cell culture supports and as such they have been studied in terms of their impact on cell adhesion and differentiation.[33] Cells on a linearly patterned pDR1M substrate were elongated with smaller nuclei whereas cells on a flat or grid patterned substrate were found to have a nucleus with a volume 400 μm^3 larger. Micropatterned surfaces were also shown to increase the elastic modulus of cell bodies.[33]

1.2 Molecular Glasses

1.2.1 Introduction to Molecular Glasses

Amorphous solids do not possess the characteristic molecular order found in a crystal. While polymers are often employed as amorphous materials, small molecules that are glass formers, called molecular glasses, are an alternative class of non-crystalline solids whose use offers several advantages. As compared to polymers, they have a more reproducible behaviour, and are usually easier to purify, characterize and process because of their monodisperse nature and smaller size.[34] In addition, they are homogeneous and formed of a single pure component. While small molecules tend to readily crystallize, it is possible to favour glass formation by tuning their structure so that they can assume different conformations of similar energy, can interact weakly with other molecules in proximity, and adopt a non-planar, irregular shape.[23] Like amorphous polymers, molecular glasses are materials that undergo a phase transition from the glassy to viscous state when they are heated above their glass transition temperature (Tg), and once cooled, return to their glassy state. Molecular glasses are thermodynamically unstable

because they continue to relax to a more stable energy state, where a local free energy minimum can be found.[35] However, they are mechanically stable because this relaxation is extremely slow compared to the time scale of experimental measurement.[35] Molecular glasses are used in a variety of applications such as, organic light-emitting diodes (OLEDs), photonic devices, electronic devices and optoelectronic devices, as shown in Figure 1.13.[36] They are also used in the pharmaceutical industry and as biosensors.[13]

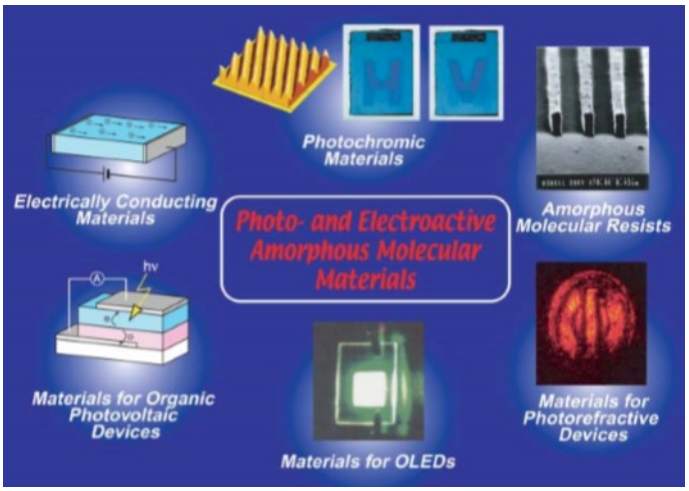

Figure 1.13: Examples of applications that employ molecular glasses. Reproduced with permission from ref 36 Copyright (2014) Royal Society of Chemistry.

A broad range of molecules have been prepared as molecular glasses. Examples include derivatives of tetraarylmethane, dithienylethene, azobenzene, oxadiazole, silole, benzimidazole, as well as boron containing compounds.[36] Structural examples of a few cores of glass forming molecules are provided in Figure 1.14. Salts have also been prepared as ionic molecular glasses. Of interest to this project is the work done by Lebel and coworkers with triazine based glasses, which will be discussed in greater detail in section 1.3.3.

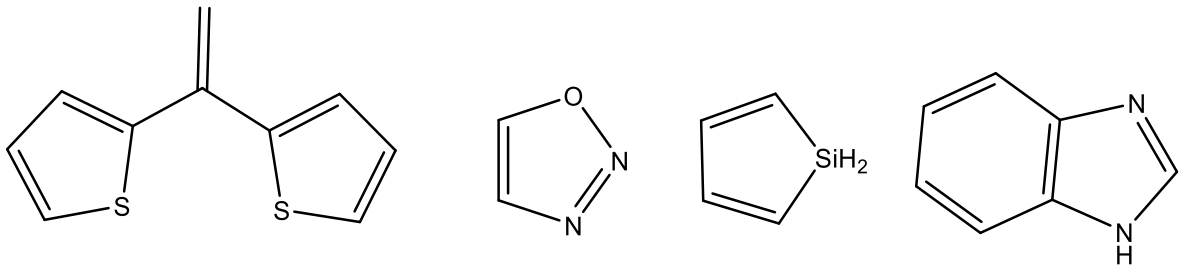

Figure 1.14: Examples of various cores of glass forming molecules. From left to right, dithienylethene, 1,2,3-oxadiazole, silole and benzimidazole.

1.2.2 Glass Forming Ability

The propensity of molecules to form molecular glasses is known as the glass forming ability, GFA. The GFA of a compound can be described by its thermal behaviour during cooling from the melt state.[37] The slowest cooling rate that can be used so that crystallization does not occur is known as the critical cooling rate.[37] When the cooling rate is fast relative to the crystal growth kinetics or when the nucleation process is inefficient, vitrification of the supercooled liquid occurs instead of crystallization.[37] A study on glass forming ability showed several factors that impact crystallization. The formation of molecular aggregates, for instance via hydrogen bonds, was found to hinder crystallization of organic compounds when they are maintained through the glass transition.[37] The aggregates impede the supercooled amorphous phase from reorganizing into the crystalline phase during cooling.[37] To make an amorphous glass, it is preferable to have an increased number of conformers with a nonplanar molecular structure.[38] Using bulky and heavy substituents for a larger molecular size also helps maintain kinetic stability of the glassy state against crystallization.[38] Formation of the glassy state can also be aided by making crystal packing more difficult. This can be accomplished by adding long alkyl chains to the molecule to increase conformational freedom, by adding bulky and irregularly shaped groups to prevent interactions between molecules, by reducing the degree of symmetry, or by using several similar groups on molecules to form multiple intermolecular interaction patterns that interfere with ordered crystal packing.[39]

1.3 Azo Molecular Glasses

1.3.1 Overview on Azo Molecular Glasses

Azobenzene derivatives are an intriguing category of molecular glasses because they appear to present the properties of amorphous materials both above and below their bulk Tg when they are irradiated.[6] Shirota and coworkers have published numerous works on azo based molecular glasses. In his review of amorphous molecular materials, he outlines research done on the properties and structures of glasses for various applications. His group prepared a large series of azobenzene based thermally stable molecular glasses with photochromic character both as films and in solution.[36] The molecules were functionalized with polar substituents as well as biphenyl and fluorenyl groups to act as the rigid moieties for increasing Tg. In all of the compounds prepared, trans-cis photoisomerization under 450 nm irradiation followed by thermal isomerization back to the trans state after cessation of irradiation was observed.[36] Cis-trans isomerization was also induced upon irradiation with 500 nm light. In measuring the quantity of cis isomers in the photostationary state, it was concluded that molecules in amorphous films cannot be completely isomerized due to a lack of free volume. This was supported by the observation of a larger fraction in the cis state in solution than in film. Substituting the phenyl groups of the azo chromophore with diarylamino groups yielded a lower cis isomer fraction, which coincided with a decrease of photoisomerization with increasing molecular size.[36] Shirota et al. also studied the kinetics of photoisomerization. The thermal relaxation followed first order kinetics only in solution.[40] In films, a fast process and a slow process were present where the rate of the slow process was similar to the rate of relaxation in solution, and the fast component was two orders of magnitude greater. Figure 1.15 shows the observed relaxation curve of the amorphous film. The two-part process was attributed to the existence of confined cis isomers that relax faster than structurally relaxed isomers. Prolonging the irradiation time allowed the free volume to increase through repetitive isomerization leading to a decrease in the fast component.[40] One of the compounds used in this study, 4-[bis(9,9-dimethylfluorene-2-yl)amino] azobenzene, has also been used to make an optical waveguide switch, as its refractive index is effectively changed upon UV or visible irradiation and because it is stable as a glass above ambient temperature without being mixed with a polymer.[41]

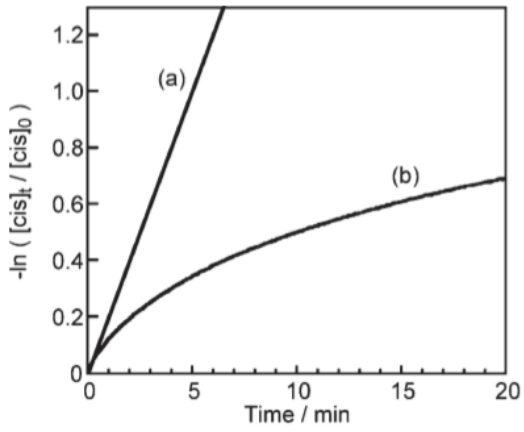

Figure 1.15: First-order relaxation plot of 4,4′-bis[bis(4-methylphenyl)amino]azobenzene (BBMAB) during cis-trans isomerization in toluene solution (a) and as an amorphous film (b) at 30 °C. Reproduced with permission from ref 40 Copyright (2000) Royal Society of Chemistry.

Since azo polymers have often been used in surface relief grating formation, the process has also been studied with azo glasses. Shirota and coworkers were able to make stable SRG's with their molecules and concluded that the presence of a polymer backbone is not necessary to make gratings.[36] Of the compounds tested, SRG formation was quicker for molecular glasses than for the analogous polymer, which was attributed to easier mass transport with the molecular glass.[36] The group has also compared SRG formation for cyano (Tg of 116 °C) and nitro (Tg of 117 °C) substituted azobenzenes from the parent compound 4-[bis(9,9-dimethylfluoren-2-yl)amino]azobenzene (Tg of 97 °C).[42] The cis fraction in the photostationary state was 0.48 for the parent compound, 0.33 for the cyano-substituted azo, and 0.14 for the nitro-substituted azo.[42] This decrease was attributed to the isomerization needing a larger volume due to the size of the substituting groups, lowering the quantum yield of trans-cis photoisomerization.[42] Figure 1.16 compares the absorption spectra of both films before irradiation and in the photostationary state. Films with the cyano substitution formed SRGs with a modulation depth similar to that of the parent compound that was greater than that of those inscribed with the nitro substitution. Increasing the Tg of the material through substitution was concluded to improve its performance

in SRG formation given the similarity in pattern size made as compared to the parent compound, despite the larger volume requirement for isomerization.[42]

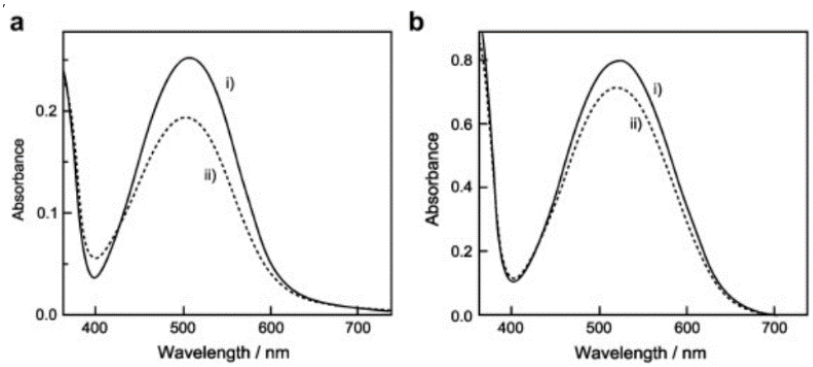

Figure 1.16: Absorption spectra of the cyano-substituted (a) and nitro-substituted (b) azo compounds prior to irradiation i) and in the photostationary state ii). Reproduced with permission from ref 42 Copyright (2010) Elsevier Inc.

Lagugné-Labarthet and coworkers have used photoinduced birefringence measurements to study molecular orientation in push-pull azo derivatives with a triarylaminoazo core.[43] The nine thin films prepared showed lower maximal and remnant birefringence than the reference polymer, pDR1M. However, the films with a tBuCN or $tBuNO_2$ substitution showed increased rate constants for the fast orientation component because the movement of their azo groups was not limited by a polymer backbone. The thin films with the fastest orientation had the lowest remnant birefringence which was attributed to angular redistribution of the trans isomers dominating the relaxation of the films. Molecules with a carbazole substitution showed less orientation but higher residual anisotropy than pDR1M as well as faster response times. Plasticization of the thin films was hypothesized as the cause of the observed increase in the birefringence plateau after each irradiation cycle of the $CarbCO_2Me$ compound. The authors concluded that azo compounds with small molecules, as opposed to polymers, have faster switching dynamics that can be tuned by the choice of the electron donating group.[43]

Nakano et al. have recently observed photoinduced shape changes in mixed molecular glass particles that coincide with structures observed in azobenzene-based single molecular glass particles.[44] Figure 1.17 shows that upon irradiation, the particles adopted a string-like

structure along the polarization direction of the incident laser beam, with the mixed particles elongating faster than the single component particles. The faster elongation was attributed to the increase in Tg of the sample upon mixing. It was noted that the effect of increasing Tg saturated at a Tg in the range of 50-60 °C, and that the elongation is facilitated when the ratio of mixed particles used increases the rate of trans-cis-trans isomerization in the system. Elongation was effective when using a ratio of 85 % single photochromic particles (4-[bis(4-methylphenyl)amino]azobenzene) with 15 % photochemically inert particles (4,4′,4″-tris[3-methylphenyl(phenyl)amino]azobenzene).[44]

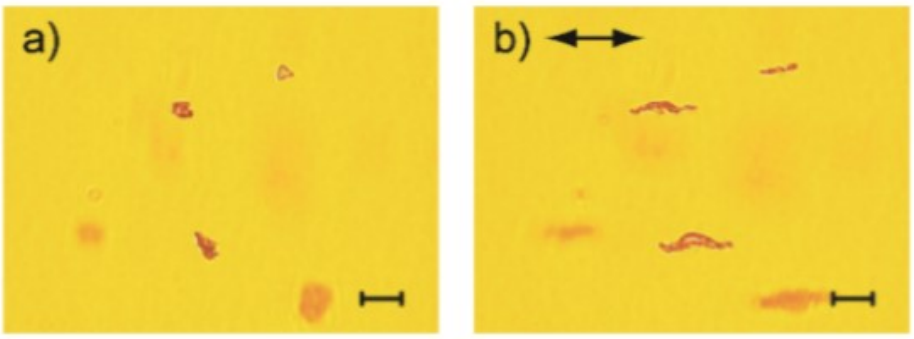

Figure 1.17: Photoinduced particle elongation observed for a mixture of 85 % 4-[bis(4-methylphenyl)amino]azobenzene and 15 % 4,4′,4″-tris[3-methylphenyl(phenyl)amino] azobenzene in agar gel prior to (a) and after 60 min irradiation with a 488 nm (15 mW or 1.7 W/cm^2) linearly polarized laser beam. Reproduced with permission from ref 44 Copyright (2018) American Chemical Society.

Controlling the Tg of a molecular glass is paramount to its suitability for a specific application. The Tg of amorphous glasses can be described by a change in density of the material along with a specific heat capacity change due to the onset of molecular movement.[36] There are several ways in which to increase the Tg such as adding a rigid moiety with a high activation energy barrier between the possible conformers, increasing the molecular size and weight (e.g. adding heavy substituents), and introducing intermolecular interactions (e.g. hydrogen bonding and dipolar interactions).[38] An application that illustrates the importance of Tg control is the formation of surface relief gratings with azo-containing molecular glasses. In one study, the

authors found that higher Tg's are better suited to SRG formation: when the Tg of the compound was 68 °C, the diffraction efficiency was near 11 %, but when the Tg was 27 °C, a grating did not form for a writing temperature of 28 °C.[45] The viscosity of the different glass materials was similar at their Tg, and it decreased with increasing temperature. Since the viscosity is related to the fluidity, it should be expected that the fluidity of a material with a higher Tg is lower, which helps the formation of SRGs by preventing collapse due to surface tension trying to smooth the surface.[45] It has also been established that for a given chromophore, there is an optimal Tg at which the diffraction efficiency is highest. This value depends on the competing factors of the chromophore's higher orientation ability and the stronger resistance of the matrix to motion at high Tg.[22]

1.3.2 Aminotriazine Molecular Glasses

Aminotriazine-based molecules can form long-lived glassy solids.[39] Lebel and coworkers have prepared a series of aminotriazine derivatives with different substitutions to determine their requirements for glass formation, as shown in Figure 1.18. There were three components of the molecules that were modified; the headgroup, the linkers and the ancillary groups. In Figure 1.18, the headgroup is labelled Y and the linkers, which serve to join the triazine core to the ancillary groups, are labelled X.

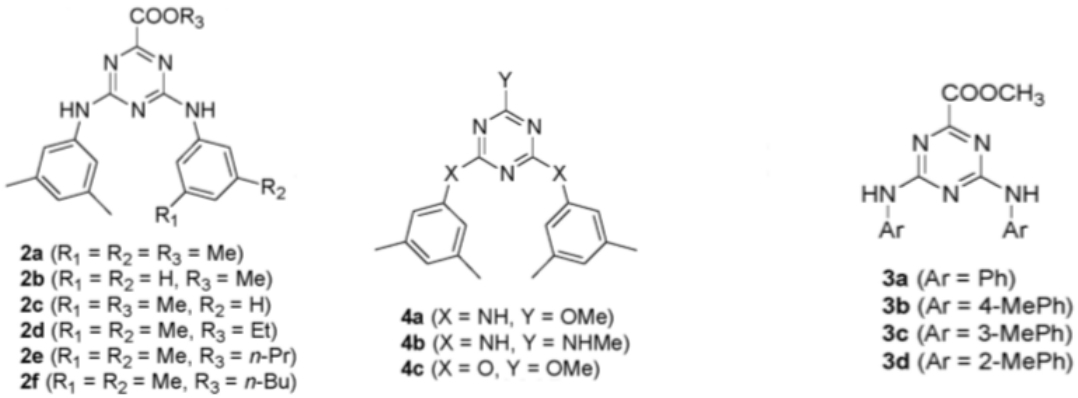

Figure 1.18: Structure of aminotriazine molecules synthesized by Lebel et al. to evaluate their glass forming ability. Reproduced with permission from ref 47 Copyright (2006) American Chemical Society.

Lebel, Pellerin and coworkers have shown that aminotriazine derivatives are a useful class of molecular glasses for study because their superb GFA permits very slow cooling rates, their Tg can be selected by the choice of headgroup, linker and ancillary groups, and they form a kinetically stable vitreous phase which prevents nucleation and crystal growth during measurement.[46] The presence of a substituent capable of hydrogen bonding is common among these glass formers.[47] These derivatives are more rigid structurally than typical molecular glasses because they have little rotational freedom, strong conjugation of the amino substituents (at the linker or headgroup positions) with the triazine ring, and higher symmetry.[34] They also have a smaller size.[23] There are two factors that contribute to their substantial kinetic resistance to crystallization and their excellent glass forming ability.[34] First, they have hydrogen bonds in the solid state that reduce mobility and raise the Tg, and second, resonance of the isomers raises the interconversion energy barrier, while ordered packing is limited by their hindered conformational equilibria.[23, 34, 46] Furthermore, the presence of one ancillary mexyl group (3,5-dimethylphenyl) prevents crystallization of numerous compounds with a wide range of other ancillary groups, from which a series of mexylaminotriazines derivatives of interest to this project were prepared.[46] A variety of ancillary groups have been tested on this core, most of which remained completely amorphous, with a 3,5 substitution providing the best GFA.[37] Mexylaminotriazines can also impart glass forming ability to the moieties they are attached to[34] and have therefore been functionalized with azos to obtain azo molecular glasses. Lebel and colleagues prepared a series of small organic molecules that easily form a long-lived amorphous phase without the risk of azo crystallization (see Figure 1.19 for synthesis) composed of a mexylaminotriazine core covalently linked to an azobenzene, where the second aromatic ring of the azobenzene was exchanged with different substituents.[23]

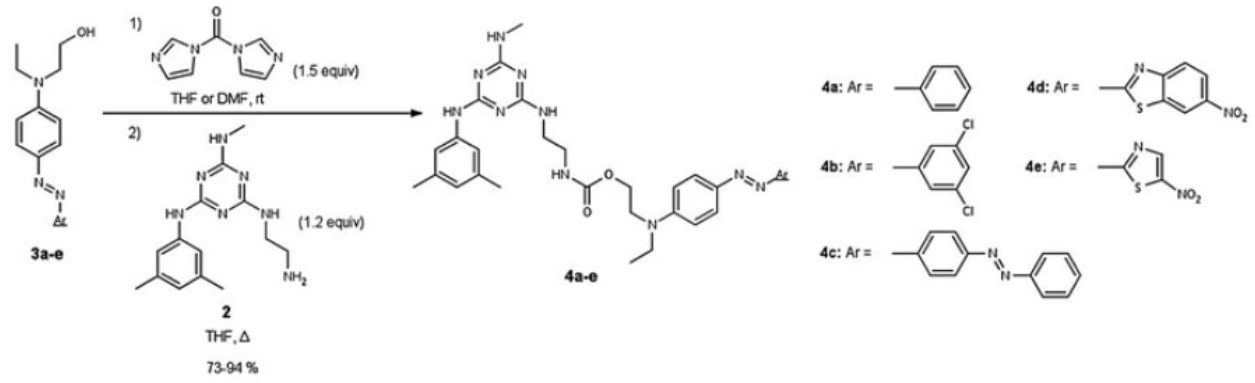

Figure 1.19: Synthesis route of the azo molecular glasses prepared by Lebel and coworkers. Reproduced with permission from ref 23 Copyright (2017) Royal Society of Chemistry.

The azo glasses resist crystallization even under an extremely slow heating of 0.5 °C/min, with all compounds showing similar Tg's. Their absorbance is similar to that of their precursor dyes, and they are soluble in several organic solvents. The glasses are able to form SRGs at numerous wavelengths, including in weakly absorbing regions.[23] This project focuses on the first azo molecule of this type that Lebel prepared, gDR1 (see figure 1.20 for structure).

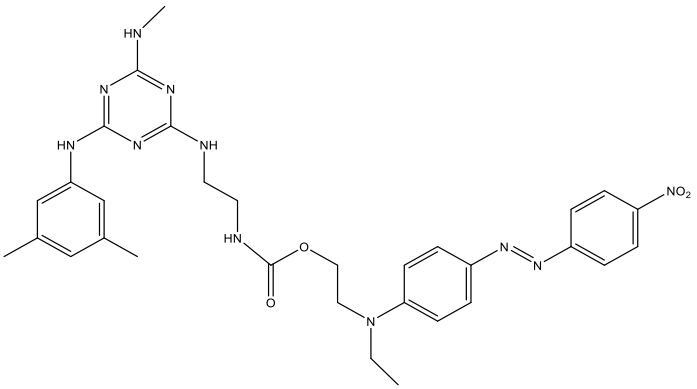

Figure 1.20: Molecular structure of gDR1.

Lebel, Sabat and coworkers have shown that gDR1 is a good nanoscale surface patterning material that effectively forms SRGs.[22] As previously mentioned, the DR1 azo chromophore undergoes rapid and repeated trans-cis-trans isomerization under irradiation.

Therefore, gDR1 is effective because under irradiation with a wavelength where the chromophore isomerizes with a high quantum yield, with fast kinetics, and with a measurable cis-content in the photostationary state, less overall absorption of light is needed for SRG formation as compared to chromophores with a higher absorbance maximum.[23] It is a useful molecule for studying photoinduced orientation and birefringence as well as photomobility in terms of the effect of the Tg and azo content independently.[22] Kirby et al. did a study where they compared SRG inscription with gDR1 and DR1-PMMA. Both the glass and polymer exhibited similar behaviour in terms of the efficiency reached for a given irradiance, 44 % at 330 mW cm^{-2} (532 nm), and the temperature at which they erased, 102 °C for the glass and 105 °C for the polymer.[34] However, the films made with gDR1 were more uniform with an absorption maximum nearer to that of pure DR1 than the DR1-PMMA films (see Figure 1.21), which was attributed to the varied polymer chain length impacting the formation of the film.[34]

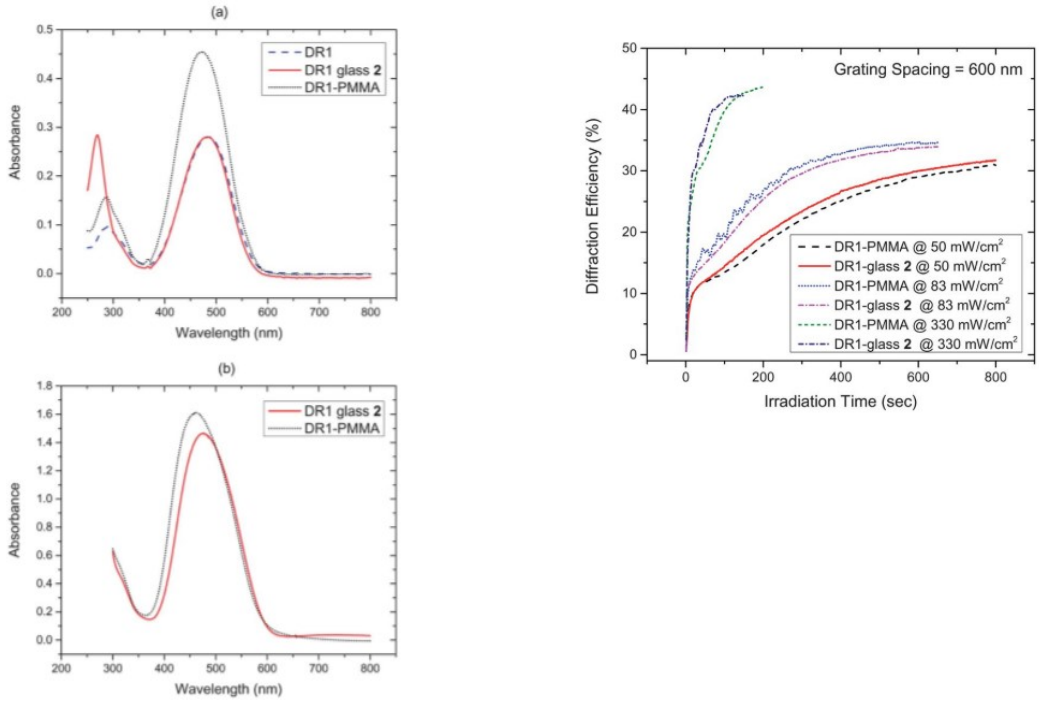

Figure 1.21: Absorption spectra (left) of pure DR1, gDR1 (0.01 mM) (shown as DR1 glass 2) and DR1-PMMA (0.0006 %wt) in CH_2Cl_2 solution (a) and of thin films of gDR1 and DR1-PMMA (b), and (right) diffraction efficiencies versus irradiation time for the thin films for different laser irradiances. Reproduced with permission from reference 34 Copyright (2016) Royal Society of Chemistry.

1.4 The Photomobility Phenomenon

1.4.1 Suggested Theories on Photomobility

As previously mentioned, photomobility is a phenomenon where molecular-scale trans-cis-trans photoisomerization can induce movement on a macroscopic scale when the material is in the glassy state, where no large-scale movement should be expected, leading to anisotropic mass transport.[22] Several theories have been suggested to explain how photomobility causes mass transport. Early on, Barrett et al. published a study with an approach suggesting that the volume difference between cis and trans isomers creates a pressure gradient.[10] In writing SRG's, they found that pressure gradients created by the light interference pattern during isomerization resulted in mass transport that was influenced by the material's viscosity, the light intensity and the free volume necessary for photoisomerization.[10] They later observed photoexpansion in azo polymer films of up to 4 % through ellipsometry.[29] The expansion was shown to be partially erasable through thermal relaxation of 1.3 % of the film thickness.[29] Another early suggestion was that mass transport results from a photoinduced directional diffusion motion.[48] In this approach, it is suggested that diffusion occurs as worm-like anisotropic motion along the axis of the molecule.[48] Teboul et al. have used molecular dynamics simulations to investigate the diffusion increase of azo materials under irradiation, reporting that isomerization occurs through a cage-breaking process leading to cooperative motion within the material.[49] In the reorientation approach, it is suggested that the photoorientation of the azo moieties creates a stress that exceeds the yield stress of the material, causing it to deform anisotropically without undergoing photosoftening.[22] Photosoftening can be understood as a decrease in some of the material's mechanical properties as a result of light exposure,[6] and is often used in tandem with the terms photofluidization and photoplasticization, depending on the material in question. Saphiannikova et al. published a study in favour of the reorientation approach with the justification that below the Tg of azo-materials there is no photofluidization transition, and therefore the materials are in a solid state allowing them to retain surface patterns in the absence of irradiation.[50] In contrast, the photofluidization approach suggests that the modulus and viscosity decrease under illumination.[22] This model was studied by measuring changes to the strain rate sensitivity of azo materials through nanoindentation. The authors found that under irradiation, the indentation strain rate of their material increased, which was accompanied by a decrease in the elastic

modulus, with no changes occurring while heating.[51] Plastic softening of the material was concluded to be dependent on the strain rate.[51] Photofluidization in polymer films was also studied by Karageorgiev et al. when they observed a light-induced isothermal transition of the material from an isotropic solid state to an anisotropic liquid state.[52]

1.4.2 Mass Transport

Photoinduced mass transport is especially used for pattern inscription, as with SRG's. A study was done where the authors controlled the deformation pattern made by pDR1A by controlling the z position of the laser focus normal to the film and the incident laser polarization.[53] The polymer moved in the polarization direction in the film plane due to light-induced anisotropic photofluidity and was pulled along the optical axis by the force of the optical gradient. Changing the z-position focus of the laser allowed forming different surfaces containing protrusions and pits of varying arrangements.[53] Mass transport occurs from bright to dark regions of the light interference pattern for amorphous molecular materials.[45] It has been suggested that there is a relationship between the frequency of isomerization cycles and the fluidity of the material: increasing the frequency of isomerization cycles makes it easier for the transportation of molecules to grow SRG's but increasing the fluidity of the material prevents forming SRG's because of surface tension trying to smooth the surface.[45] It was therefore concluded that increasing the Tg will favour SRG formation because for molecules with similar photochromic properties, the fluidity upon room temperature irradiation will decrease when the Tg is higher.[45]

In a recent work, our group studied the photoactivity of azo materials to define optimal thermal properties for SRG inscription. To do so, pure gDR1 as well as blends of gDR1 with photopassive glasses of varying Tg were used. Using mixtures of photoactive and photopassive mexylaminotriazine molecular glasses to study the effect of temperature on SRG formation provides several advantages. First, the same azo chromophore can be used for all tests, giving the same optical properties and photoactivity to all samples. Second, the relative inscription temperature can be changed by tuning the Tg of the mixture, rather than the experimental temperature, simplifying the experiment. Finally, discrepancies in molecular weight as well as dispersity issues are avoided when both the photoactive and photopassive components are

molecular glasses as opposed to polymers.[22] UV-Vis spectra were used to determine the cis half-life after irradiation by measuring the absorbance during thermal relaxation.[22] The cis content during irradiation was found to change very little when changing the Tg and azo content of a blend of gDR1 from that of pure gDR1 because under 520 nm irradiation, both the trans (π,π*) and cis (n,π*) bands are excited simultaneously, which causes fast trans-cis-trans isomerization cycles. Figure 1.22 shows the cis content and cis half-life observed for the different blends. The cis half-life was found to increase from 5 s for blends with the lowest Tgs (around 20 °C) to 70 s when the Tg exceeds 50 °C where a plateau is reached.

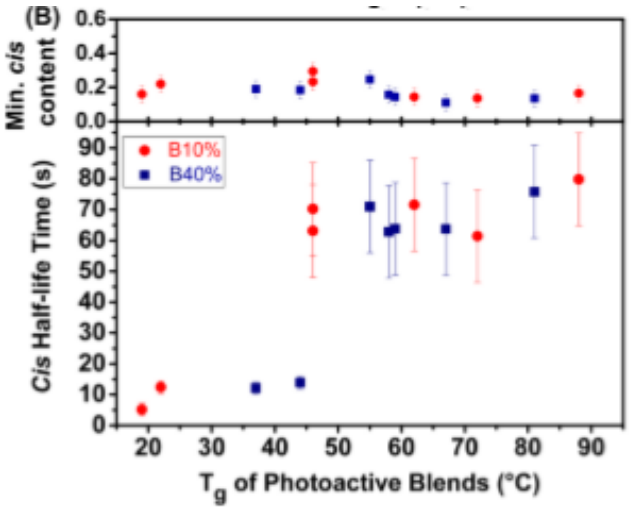

Figure 1.22: Cis half-life and minimum cis content of azo blends with 40 and 10 % gDR1 according to their glass transition temperatures (Tg). Reproduced with permission from ref 22 Copyright (2017) American Chemical Society.

The increase of half-life was attributed to the material being in a glassy state rather than a viscous one, where the free volume available for the glass to relax is smaller. An opposite trend was found in a study by Nakano et al. on azo molecular glasses, where high Tg films had higher rate constants, and it was noted that the ability of the cis isomer and matrix to form hydrogen bonds for the higher Tg blends could explain their higher lifetime. Hydrogen bonding between the trans isomer and the matrix was stated as a possible cause for all blends having a similar minimum cis content during irradiation, showing that even if the thermal relaxation is

longer, there is no accumulation of cis isomers in the high-Tg blends. Figure 1.23 shows that for blends with a 40% azo content, the diffraction efficiency after 1000 s of irradiation increased from 2.5 to 18 % with increasing Tg and reached a plateau for Tg values above 60 °C. For the blends with a 10 % azo content, the diffraction efficiency reached a maximum of 6 % and it did not continue to increase with increasing Tg. A low DE for low Tg samples was attributed to efficient thermal relaxation of the rubbery matrix. With high Tg blends, a longer inscription time was required to reach saturation because the high viscosity of the film counteracts photo-orientation of the chromophore and produces slower inscription kinetics. The optimal Tg of inscription was 45 °C for blends with a 10 % azo content and 60 °C for the 40 % blends because the blends with the 40 % azo content were better at generating motion in the high-Tg matrix. Motion of the matrix was suggested to occur through a structural relaxation process, either by generating an excess free volume during photoisomerization or by imposing more stress on the matrix. The diffraction efficiency was maximal at the optimal Tg because isotropic viscous flow of the matrix under irradiation is less likely at higher Tg (see Figure 1.23).

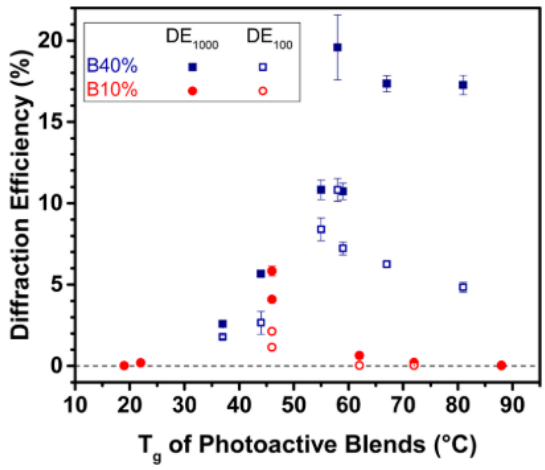

Figure 1.23: Diffraction efficiency of photoactive blends with 10 and 40 % gDR1 according to their glass transition temperatures (Tg) after 100 s (empty symbols) and 1000 s (full symbols) of irradiation. Reproduced with permission from ref 22 Copyright (2017) American Chemical Society.

When the Tg of the material exceeds the optimal Tg, photoinduced mass transport is prevented by the high viscosity of the material. There is an implied kinetic limiting factor when

the Tg is greater than the optimal value because the matrix must be able to be pushed anisotropically or adapt to the azo's angular redistribution during the isomerization.[22] Therefore, when the Tg becomes too high for the azo to generate anisotropic free volume or to put stress on the matrix to provoke an anisotropic motion, it will instead return to its original angular distribution after the trans-cis-trans cycle instead of inscribing an SRG.[22] Having a high azo content and a Tg that is close to the optimal Tg for inscription of DR1 derived azomaterials makes gDR1 an excellent candidate for SRG inscription.[22, 34]

1.4.3 Photosoftening

In an experiment on photosoftening, using nanoindentation, the hardness and elastic modulus of pDR1M's SRGs was shown to increase as a result of irradiation which was associated with an increase of the polymer density.[54] A more recent inquest into the topic used pDR1A films to investigate photoinduced mechanical changes. The study showed that visible light irradiation leading to repetitive trans-cis-trans isomerization softened the azopolymer while UV irradiation hardened the polymer through trans to cis conversion.[55] The authors found that under 532 nm illumination, the strain rate sensitivity of the material increased by 81% during a nanoindentation experiment.

In a paper published by our group on photoplasticization using gDR1 and pDR1A, irradiation was shown to generate a molecular environment similar to that generated by heating but with changes that were heterogeneous at the submolecular scale.[6] An effective temperature was established to gain insight into the molecular environment under irradiation by analysis of infrared spectra. The effective temperature corresponds to the temperature at which the sample needs to be heated to experience the same molecular environment as it does under irradiation. The effective temperature is determined by associating the band position of a given part of the material at a given temperature to the band position under irradiation. This was used to establish the local effective temperature of different regions of the molecule that was related to the local free volume and was suggested as a cause for photoinduced motion below Tg. Figure 1.24 shows the effective temperature of different parts of gDR1 and pDR1A.

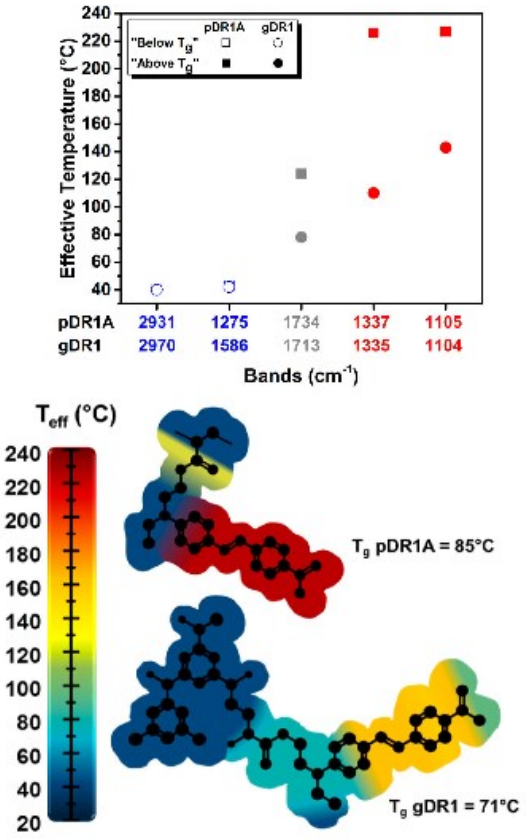

Figure 1.24: Effective temperature gradient of gDR1 and pDR1A felt under 520 nm irradiation (bottom panel) as established using infrared bands associated with the azo (red), spacer (grey) and backbone (blue) moieties of the compounds (top panel). Reproduced with permission from ref 6 Copyright (2015) American Chemical Society.

It was suggested that the generation of free volume is the cause for the band shifts observed under illumination and during heating, because it decreases the strength of intermolecular interactions by allowing freedom to move in the conformational space and by increasing the average intermolecular distance. During this experiment, the free volume under irradiation increased the most around the azo moiety and to a decreasing extent with distance from it. In contrast, upon heating, the increase in free volume is experienced similarly by the whole molecule. These observations led to the conclusion that illumination causes some parts of the molecule to experience the same local environment they would if heated above the bulk

Tg even though the sample is held at a temperature well below Tg. These results show that under irradiation below Tg, gDR1 is partly in a glassy state, at its triazine core, and partly in a viscous-like state, around its spacer and azo, which was said to confirm the generation of soft regions in the material. It was suggested that phototransport could be facilitated by making a bulkier azobenzene substituent because it could increase the molecule's effective temperature gradient and generate a larger free volume during irradiation.[6] A photoinduced local temperature increase in a monolayer azo glass has also been observed by Fang et al. where an effective local temperature as high as 800 K was measured under irradiation for the azo group with changes to viscosity equivalent to changes observed upon heating above Tg.[56]

1.5 Project Objective and Content of the Thesis

The main objective of this project is to determine if the phenomenon of photomobility is a result of light-stimulated structural relaxation. gDR1 is the primary molecular glass studied, with an analogous photopassive molecular glass (g70), and polymer pDR1A serving as control samples. The goal of this project was to investigate the role of enthalpic relaxation in photomobility. When photoisomerization occurs, gDR1 undergoes an increase in free volume. This free volume increase should be related to an increase in enthalpy in the system, a phenomenon that has not been explored to our knowledge. Four characterization techniques were chosen to measure changes in the properties of the material during and following irradiation. UV-visible spectroscopy is used to determine the minimum cis content that can be reached in the photostationary state under irradiation using four different wavelengths that fall within the absorbing region of the material. Two of the wavelengths, 520 and 450 nm, are near the maximum absorption of the trans band, while 365 nm is closer to the maximum absorption of the cis isomer, and 405 nm is weakly absorbed by both. Continuing with the work previously done by the Pellerin group, where the molecular environment of gDR1 under irradiation below Tg was tested,[6] IR spectroscopy is used to determine the effective temperature of the backbone, spacer and azo of the material under irradiation with each of these wavelengths. The previous work was limited to the effect of 520 nm irradiation. In the present work, multiple irradiation wavelengths are used to understand the effect of the cis content in the photostationary state and of the efficiency of trans-cis-trans cycling. The relaxation process of each group is measured to

obtain insight on the kinetics of relaxation. Ellipsometry measurements are taken to confirm that photoexpansion of the film occurs by measuring the change in film thickness under irradiation, as well as to monitor the relaxation of the film at the macroscopic scale. The enthalpy relaxation associated with trans-cis-trans cycling is measured by differential scanning calorimetry. To do so, samples are first annealed for various times and at different temperatures to measure the change in enthalpy that occurs upon structural relaxation. The procedure is then repeated with samples that are irradiated before or after the annealing to reveal the effects of photoisomerization.

Chapter 1 contains an introduction to the study of azobenzene-based molecules followed by an overview of the use of molecular glasses to study photoinduced motion. Chapter 2 describes the experimental procedures followed for sample preparation and for each of the laboratory techniques used. Chapter 3 presents the results and discussion of the findings of this project. Finally, Chapter 4 presents the conclusions of this project and holds perspectives for future topics of study.

Chapter 2

Experimental Section

2.1 Materials

gDR1 was obtained from our collaborator Prof. Olivier Lebel at the Royal Military College of Canada. It was synthesized and purified following his published procedure.[34] Dichloromethane (CH_2Cl_2) was used as the solvent for solution preparation. Glass microscopy slides were used as the substrate for UV-Visible measurements while silicon wafers (UniversityWafer) were used for ellipsometry. Reference measurements were taken for selected experiments using molecular glass g70 (also synthesized by Prof. Lebel) and polymer pDR1A (obtained from Sigma Aldrich). The solvent used was chloroform ($CHCl_3$).

2.2 UV-Visible Spectroscopy

An Ocean Optics USB2000+ fiber-coupled spectrophotometer with a DH-mini light source was used to take UV-Vis spectra of gDR1 prior to and following irradiation with a collimated LED source (Prizmatix FC5Multichannel LED) at 520 nm (31.8 mW/cm^2), 450 nm (94.2 mW/cm^2), 405 nm (31.2 mW/cm^2), and 365 nm (50.5 mW/cm^2). Samples were prepared by spin-coating (2000 rpm, 60 s) gDR1 dissolved in CH_2Cl_2 (2.2 mg/mL) onto glass microscopy slides. The slides were cut into squares (approximately 3x3 cm^2) and cleaned with acetone. Spectra were measured every second for 2 min of irradiation followed by 2 min of thermal relaxation. The integration time used was 10 ms, averaging 100 scans, with a boxcar halfwidth of 5. A homemade black box with a sample holder and a light source holder was used. OPUS 6.0 software (Bruker Optics) was used to determine the absorbance maxima of the spectra. The maximum of the bands was determined relative to zero.

2.3 Infrared Spectroscopy

A Tensor 27 FT-IR spectrometer (Bruker Optics) with a liquid nitrogen-cooled MCT (Mercury-Cadmium-Telluride) detector was used along with a Heated Golden Gate (Specac) attenuated total reflection (ATR) accessory to record IR spectra while varying the sample

temperature and while irradiating the sample. Samples were prepared by dissolving gDR1 in CH_2Cl_2. The solution (0.4 mg/mL) was gently shaken by hand and then 50 µL were deposited on the accessory's single reflection diamond element at 40 °C. The sample was heated to 140 °C at ~40 °C/min to erase thermal history and to ensure evaporation of the solvent. The temperature was then left to stabilize during an isotherm of 3 min. A cooling ramp of 2 °C/min from 140 to 40 °C was used while recording spectra at every 2 degrees with a 4 cm^{-1} resolution and averaging 50 scans. Background spectra of the bare ATR element were measured prior to the sample following the same procedure. At 40 °C, an irradiation cycle of 2 min of darkness followed by 2 min of irradiation, repeated 3 times, followed by an additional 12 min of was accomplished with the LED source described for the UV-visible measurements, at the same wavelengths. A black box was custom-made to reproducibly hold the LED head above the sample at a constant distance for each experiment, and to keep the sample in the dark when the LED was off. OPUS 6.0 software (Bruker Optics) was used to characterize the band positions of the spectra. The peak picking was done by determining the center of gravity of selected bands with a sensitivity of 1 using the top 50 % of the bands, making the uncertainty on the band positions on the order of 0.01 cm^{-1}.

2.4 Ellipsometry

A J.A. Woollam M-2000 spectroscopic ellipsometer was used to measure the change in thickness of gDR1 thin films (approximately 20 nm thick) resulting from irradiation. Films were prepared by spin-coating (2000 rpm, 60 s) a solution of gDR1 (2.2 mg/mL) dissolved in CH_2Cl_2 (0.45 mL) onto silicon wafers. The wafers were cleaned by sonication in acetone for 15 min followed by cleaning with methanol. The thickness was measured continuously as a function of time (50 revolutions/measurement, 17 s minimum acquisition period). The thickness was first measured prior to irradiation, then under irradiation for 2 min, then for 12 min without the light during film relaxation. The LED light source was used for the irradiation with 520, 405 and 365 nm. The fitting model used to determine the thickness was made by first estimating the thickness of the film in the transparent region above 700 nm to fit for the refractive index (n and k values) of the film at all wavelengths. Once the n and k values were determined they were used to build

an oscillator model describing their dispersion. The model then determined the thickness based on these measured values.

2.5 Differential Scanning Calorimetry (DSC)

A PerkinElmer DSC 8500 calorimeter with a PerkinElmer Intracooler 2P cooling accessory was used for differential scanning calorimetry measurements to determine the Tg and enthalpy relaxation associated with annealing gDR1 for varied times up to 6 hours at 40, 60 and 70 °C. The DSC was calibrated with indium using a 10 °C/min heating rate from 100 to 180 °C. Samples were prepared by directly placing the molecular glass (2 mg) in a standard aluminum DSC pan. The Tg was measured as the half height of the heat capacity jump of the heating scans. The samples were first heated from 50 to 135 °C to erase thermal history. They were then cooled ballistically (as fast as possible) to a given temperature and annealed for a selected time. They were then ballistically cooled to 0 °C from the annealing temperature. Two heating scans were then measured from 0 to 135 °C while heating at 10 °C/min. The samples were ballistically cooled to 0 °C prior to measuring the second heating scan. Upon each step of reaching 0 or 135 °C the samples underwent an isotherm of 3 min. The enthalpy relaxation was determined by measuring the area of the peak resulting from subtracting the second heating scan, where the thermal history of the sample had been erased, from the first heating scan, where the sample had undergone annealing. Samples were also measured after undergoing 520 and 405 nm irradiation with the same LED source as above to determine the extent to which the annealing could be erased. The source was held with the black box used for IR measurements with care to ensure the LED head was positioned above the sample pan in the DSC. The samples were first heated to 135 °C to melt the glass into a film so that unlidded pans could be used in the DSC without spilling the sample. Irradiation was done either prior to or immediately following the annealing. The two heating scans were then measured as before.

Chapter 3

Results and Discussion

3.1 UV-Visible Spectroscopy

gDR1 undergoes repetitive trans-cis-trans isomerization under irradiation in the UV or visible range which can be seen by comparing its absorption spectra prior to irradiation and during thermal relaxation after irradiation. Figure 3.1A shows the absorption spectra of gDR1 prior to irradiation, immediately after irradiation with 520 nm light (time 0) and after 120 seconds of thermal relaxation. At this wavelength, both the trans and cis isomers absorb, resulting in fast cycling between isomers. Under irradiation, the trans (π,π*) absorbance band at 480 nm decreases in intensity.[22] This is accompanied by the small growth of the cis (n,π*) band near 400 nm. When the light is turned off, the cis isomers thermally relax back to the trans state and the absorbance of the trans (π,π*) band gradually increases towards its initial value.

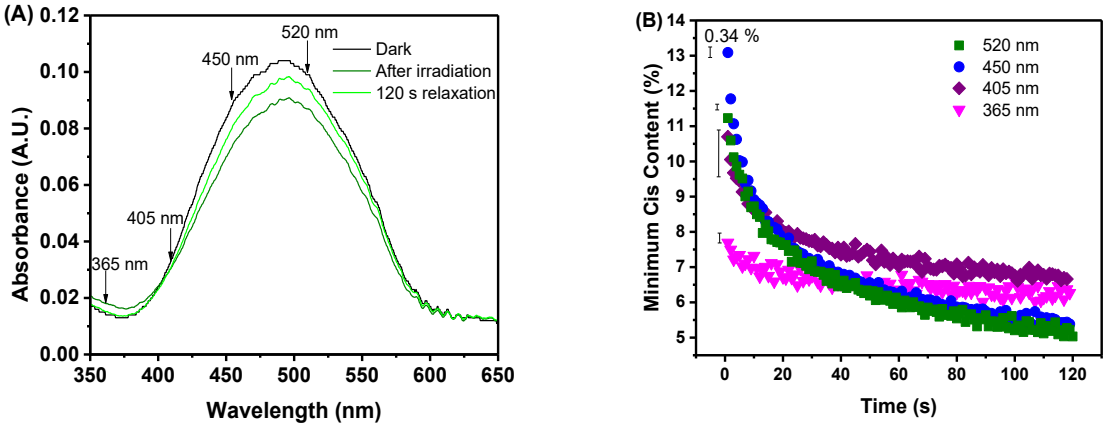

Figure 3.1: (A) Absorption spectra of gDR1 before irradiation, immediately following irradiation with 520 nm light, and after relaxing in the dark for 120 s. (B) Minimum cis content of gDR1 during thermal relaxation following irradiation with 520, 450, 405 and 365 nm light.

By measuring the absorbance of the trans (π,π*) band during thermal relaxation, it is possible to determine the minimum cis content of gDR1 using Eq. 3.1:[22]

$$min.cis\ content = (1 - \left(\frac{A_t}{A_{initial}}\right))x\ 100 \quad (3.1)$$

where A_t is the absorbance for a given time of thermal relaxation, and $A_{initial}$ is the absorbance prior to irradiation.

Figure 3.1B compares the minimum cis content during 2 min of thermal relaxation after irradiation with LED light of various wavelengths. Each of the wavelengths used result in trans-cis and cis-trans photoisomerization for a push-pull azobenzene such as DR1, which explains the low cis content observed.[6] The highest minimum cis content is reached under 450 nm irradiation (94.2 mW/cm^2) at 13 %, followed by 520 nm irradiation (31.8 mW/cm^2) with 11 %, with the relaxation curves for these two wavelengths overlapping. Under 405 nm (31.2 mW/cm^2) irradiation, the cis content reaches 10.7 %, while 365 nm (50.5 mW/cm^2) irradiation leads to the smallest value of 7.7 %. The observed cis contents can be explained by the proximity of the irradiation wavelength to the maximum of the trans absorption band, which favors trans-cis isomerization, and to the maximum of the cis absorption band, which favors to reverse cis-trans isomerization and therefore increases the cycling efficiency of photoisomerization. Figure 3.2 shows a calculated spectrum of DR1 in the trans and cis conformation in vacuum. The TD-DFT calculation was conducted in Gaussian 16 with the B3LYP functional and the 6-31+G(d,p) basis set. The irradiation wavelengths of 520 and 450 nm are near the maximum of the trans band (480 nm), while 405 and 365 nm wavelengths are much less absorbed by the trans isomers. The wavelengths closer to the trans absorbance band maximum lead to more trans-cis isomerization. The minimum cis content under photostationary state is therefore higher for 520 and 450 nm irradiation. The latter gives the highest cis content value in part because of a higher irradiance of the LED. These two irradiation wavelengths nevertheless yield efficient trans-cis-trans cycling because of significant cis absorption in the same spectral range. The lower trans absorption for 405 and 365 nm irradiation leads to lower cis content, but it can be noted that the cis content is higher than what could be expected when considering the relative absorbance at these wavelengths. This is a consequence of a difference in trans-cis-trans cycling efficiency. In particular, the 405 nm light falls between the two cis absorption bands in the calculated spectrum, suggesting that the photochemical cis-trans reaction is inefficient. A comparison of

the ratio of cis content over absorbance for each irradiation wavelength can be used as an indication of the relative efficiency of cis isomer formation for the same light absorption. When gDR1 absorbs 450 nm light it forms the cis isomer 1.3 times (calculated as efficiency of 450 nm / efficiency of 520 nm) more efficiently than 520 nm, while 405 nm and 365 nm form the isomer 3.3 and 5 times more efficiently than 520 nm. Irradiation at 520 nm therefore yields the most efficient trans-cis-trans isomerization. On the other hand, 405 and 365 nm cause less efficient cycling. Interestingly, a similar cis content is observed for 520 and 405 nm light because the faster cycling at 520 nm limits the cis content in the photostationary state, while the less efficient cycling with 405 nm produces a relatively large cis content despite the low trans absorption. Consequently, these two irradiation wavelengths are especially useful to discriminate the effects of cis content is trans-cis-trans cycling on the photomobility of gDR1.

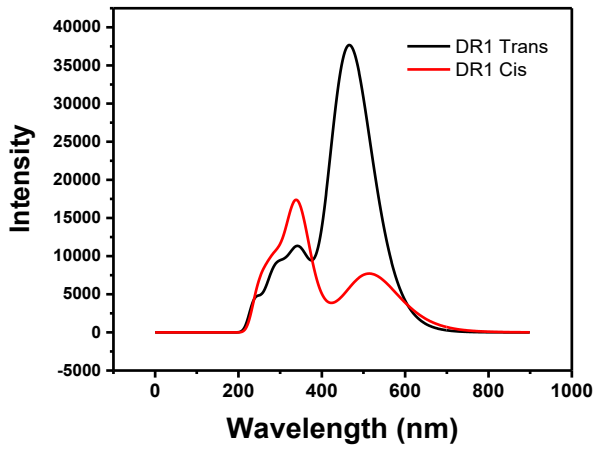

Figure 3.2: Calculated absorption spectrum of DR1 under vacuum.

As shown by the shape of the curves in Figure 3.1B, thermal relaxation from the cis to trans form is faster and more complete after irradiation with the wavelengths that produce more efficient cycling. After the relaxation, the cis content falls to 5 % for 520 nm irradiation, 5.4 % for 450 nm and 6.7 % for 405 nm, a decrease of 6, 7.6 and 4 % respectively, while for 365 nm it drops to 6.3 %, a change of only 1.4 %. The cis content for 520 nm irradiation was measured for a longer time period and reaches 3.9 % after 12 min of relaxation. The efficiency of thermal relaxation after irradiation can also be compared by looking at the remaining fraction of cis

isomers after 2 min of relaxation. The residual cis content is 45 % for 520 nm, 41.5 % for 450 nm, 62 % for 405 nm and 82.4 % for 365 nm. In other words, contrary to our initial expectation, the cis-trans thermal relaxation is affected by the irradiation wavelength, most likely due to the difference in photochemical trans-cis-trans cycling during irradiation.

By fitting the thermal relaxation curves, it is possible to obtain information pertaining to the rate of relaxation. As seen by the shape of the curves in Figure 3.1B, thermal relaxation follows an exponential decay. For push-pull type azo's such as gDR1, the best fit is given by a biexponential consisting of an initial fast process followed by a second slower relaxation process.[29] Numerous works have stated that the presence of two processes is a consequence of the existence of two types of environments resulting from the inhomogeneous distribution of free volume in the matrix.[57-60] The fast process represents the relaxation of cis isomers that are trapped in a strained environment with less free volume and thus relax more quickly to the trans state. On the other hand, the slow process represents the relaxation of cis isomers in a relaxed environment because of a greater free volume. It is expected that the thermal relaxation be on the order of seconds because of the low cis-isomer concentration in the photostationary state.[6] The fitting equation (3.2) used is as follows:

$$min.\,cis\ content = y_0 + A_1 exp^{-(\frac{t}{\tau_1})} + A_2 exp^{-(\frac{t}{\tau_2})} \quad (3.2)$$

where y_0 is the cis content plateau reached after the relaxation, A_1 and A_2 are the weighing constants for the first and second process, τ_1 and τ_2 are the time constants of the fast and slow process, and t is the relaxation time in seconds. Table 3.1 contains the thermal relaxation values obtained for both processes. In all cases, y_0 is approximately equivalent to the minimum cis value reached after relaxation, as should be expected because it is related to the percentage of isomers that have not relaxed (a possible out-of-plane photoinduced orientation may also contribute to the y_0 values even though the irradiation was conducted with unpolarized light impinging the sample with oblique incidence to minimize this effect). With a successful fitting, the sum of y_0, A_1, and A_2 should be equivalent to the maximum cis value reached, as observed here. For all wavelengths, t_2 is an order of magnitude greater than t_1, except with 365 nm where it is two orders of magnitude greater. The margin of error (standard deviation of the fitting values obtained for triplicates) is reasonably small except for 365 nm, which is likely a result of the

deviation from the exponential decay in the relaxation curve due to the much slower relaxation. The results indicate that when the irradiation generates a higher cis content with efficient cycling (520 and 450 nm), and therefore creates more free volume in the glassy matrix, the cis isomers can relax faster to the trans state because they have more room to do so. By contrast, irradiation at 405 and 365 nm produces limited cycling and results in an increasing weight of the y_0 term which can be associated with cis isomers kinetically trapped in a rigid matrix.

Table 3.1: Thermal relaxation values obtained from fitting the cis content relaxation curves with equation 3.2 (uncertainties are shown in italics).

Wavelength, nm	y_0, %	A_1	τ_1, s	A_2	τ_2, s	Min cis content, %	Cis content after relaxation, %	Cis change, %
520 (12 min)	3.7	4.4	20.6	2.6	220	11	3.4	7.3
	0.33	*0.3*	*0.5*	*0.1*	*18*	*0.5*	*0.8*	
520	4.8	2.9	6.5	3.9	51	11	5.0	6
	0.3	*0.2*	*0.7*	*0.2*	*1*	*0.5*	*0.4*	
450	5.2	4.5	3.7	4.3	40	13	5.4	7.6
	0.4	*0.5*	*0.6*	*0.3*	*4*	*1*	*0.3*	
405	6.6	2.2	4.3	2.3	41	10.7	6.7	4
	1.5	*0.3*	*0.7*	*0.2*	*2*	*1.7*	*1.4*	
365	6.0	2	8	1.0	112	7.7	6.3	1.4
	0.1	*2*	*12*	*0.2*	*123*	*0.05*	*0.1*	

3.2 Infrared Spectroscopy

Previous work by our group presented the concept of effective temperature (T_{eff}) using IR spectroscopy to correlate the effects of temperature and irradiation on the molecular environment of azo-containing amorphous compounds.[6] By overlaying the band shift of a given band of the molecule measured at various temperatures during a cooling ramp to the band shift under irradiation at a fixed temperature, it is possible to gain insight as to what temperature the material must be heated to homogenously experience the same molecular environment it does under irradiation. Figure 3.3 shows the band shift of an azo band (1335 cm^{-1} NO_2 symmetric stretching band) when cooling from 140 to 40 °C, and during an irradiation cycle of two minutes

in the dark followed by two minutes irradiation repeated three times, followed by twelve minutes of thermal relaxation in the dark. The cooling curve shown is an average of three repeated measurements to ensure that each effective temperature measured is based on the same reference cooling ramp.

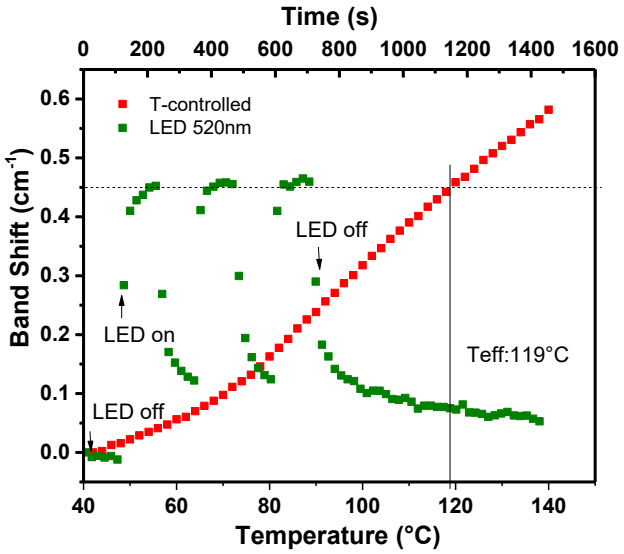

Figure 3.3: Band shift of the azo band (1335 cm^{-1}) under irradiation at 520 nm (green) overlaid with its band shift as a function of temperature (red) to determine the effective temperature.

Figure 3.3 shows that, under irradiation, the effective temperature of the azo group increases. When the light source is turned off, it slowly relaxes back towards its initial value. During the irradiation, the band shift and the effective temperature tend toward a maximum value and plateau, respectively. It can also be observed that the slope of the temperature-controlled curve changes at the Tg (71 °C). Fitting both segments of the curve with a linear equation allows converting each band shift measured in the irradiation cycle into an effective temperature. The band shift on the temperature-controlled curve at Tg is used to determine which equation of the curve to use for a given band shift. Band shifts lower than the band shift at 71 °C are plugged into the equation fitted below Tg, while band shifts above it are plugged into the curve above Tg. Figure 3.4 shows the band shift converted to an effective temperature felt by the backbone (1586 cm^{-1} triazine ring stretching), spacer (1713 cm^{-1} C=O stretching) and

the azo (1335 cm^{-1}) during the irradiation cycle with A) 520, B) 450, C) 405 and D) 365 nm light. The curves are an average of three measurements.

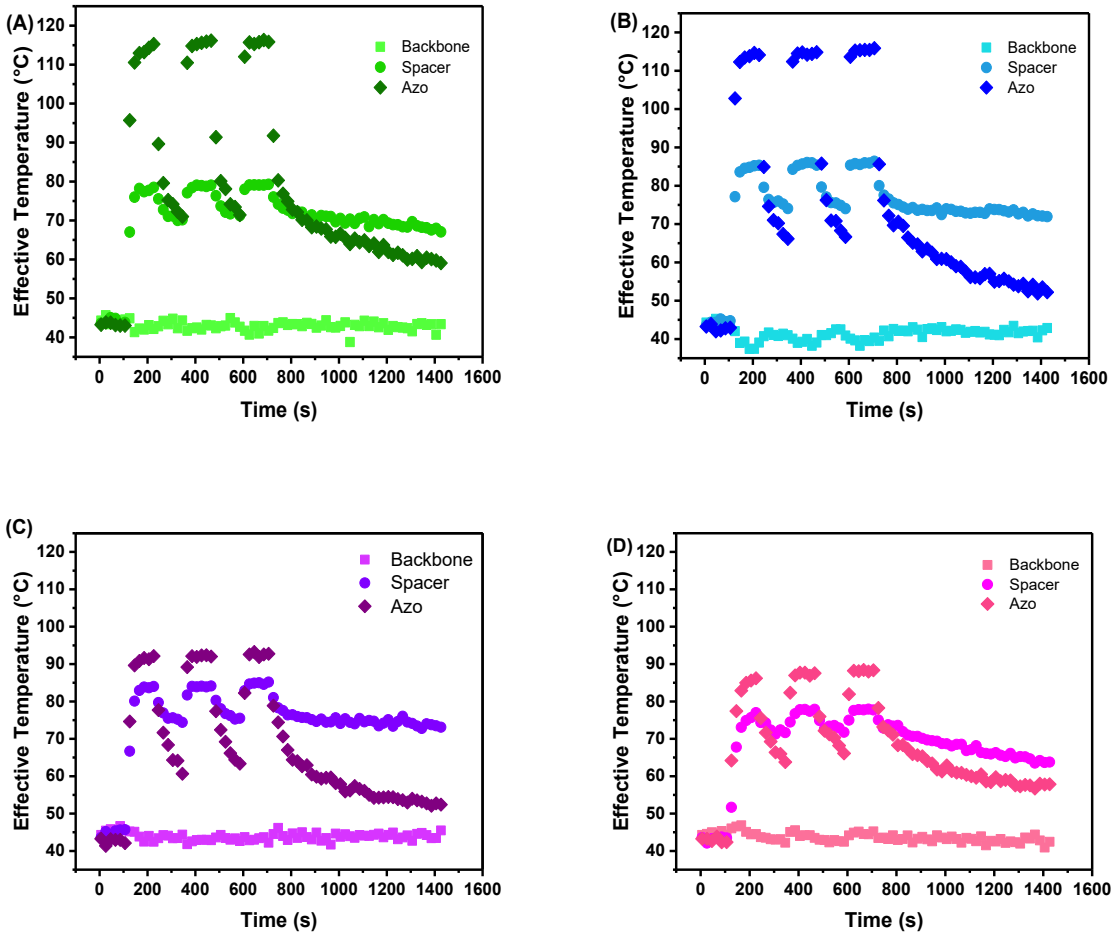

Figure 3.4: Effective temperature during the irradiation cycle with (A) 520 nm and (B) 450 nm (C) 405 nm and (D) 365 nm irradiation.

The maximum effective temperature reached under irradiation at the different wavelengths is shown in Table 3.2 as an average of multiple repetitions (3-5). The residual T_{eff} values reached after 12 min of relaxation are also reported for the azo and spacer groups.

Table 3.2: Average effective temperature (°C) of gDR1 under irradiation for selected bands (uncertainties are provided in italics).

Wavelength, nm	Effective Temperature, °C			Residual Effective Temperature, %	
	Azo (NO_2)	Spacer (C=O)	Backbone (triazine ring)	Azo	Spacer
520	116 *9*	78 *4*	46 *1*	25 *11*	69 *2*
450	113 *8*	87 *3*	45 *1*	18 *2*	70 *6*
405	92 *2*	86 *2*	44 *1*	24 5	75 9
365	88 *2*	80 *1*	44 *2*	37 *9*	63 *9*

The effective temperatures under 520 nm irradiation are 116 °C for the azo, 78 °C for the spacer, and 46 °C for the backbone. The azo experiences a larger increase in free volume than the rest of the molecule because it is where the trans-cis-trans isomerization occurs.[6] Unlike with heating where the free volume increase is expected to be the same for the molecule as a whole, with photoisomerization the free volume increases less when further from the azo groups.[6] The previous work concluded that the different effective temperatures felt along the molecule confirm that under irradiation below the bulk Tg, the backbone exhibits glassy properties ($T_{eff} < Tg$) while the spacer and azo exhibit fluid-like properties ($T_{eff} > Tg$).[6] The T_{eff} measured here are comparable to the values reported in the previous work. The spacer T_{eff} was the same, the azo T_{eff} was within the margin of error measured here, with the backbone T_{eff} 5 °C higher in the present work but still well below Tg. When writing surface relief gratings, the diffraction efficiency of gDR1 under 532 nm, close to the wavelength used here, has been shown to reach 44 %[34] because its Tg is near the optimal inscription temperature of DR1 azomaterials and because of its high azo content.[22] As observed under UV-Vis spectroscopy measurements where the cis content reached under 450 and 520 nm irradiation was similar and the trans-cis-trans cycling also appeared similar, the effective temperatures felt by the azo and the backbone groups under 450 and 520 nm irradiation are also very similar: the effective temperature reached under 450 nm is 113 °C for the azo, 87 °C for the spacer and 45 °C for the backbone. Figure 3.4C shows the results of the experiment using an irradiation wavelength of 405 nm. The

effective temperature reached with this wavelength is 92 °C for the azo, 86 °C for the spacer and 44 °C for the backbone. A much lower effective temperature felt by the azo under 405 nm light can be associated with the decreased trans-cis-trans isomerization. Indeed, as was observed in Figure 3.1B, irradiation with 520 or 405 nm light results in very similar cis contents despite the much higher absorbance at 520 nm. The effective temperature reached under 365 nm is similar to that of 405 nm: 88 °C for the azo, 80 °C for the spacer and 44 °C for the backbone. These slightly smaller T_{eff} values are likely associated with the lower apparent cycling efficiency for 365 nm than for 405 nm irradiation conditions. It is noteworthy that the values are similar in spite of the lower cis content under 365 nm irradiation (7.7 % vs. 10.7%), reinforcing the conclusion that trans-cis-trans cycling, and not cis content, is the main origin for the increase in effective temperature.

The same experiment was done using 630 nm irradiation (60.5 mW/cm^2), which is at the limit of the absorption region of gDR1. Figure 3.5 shows one of the triplicates measured for the azo group. While the azo displays a similar pattern to that observed at the other wavelengths, the band shifts of the spacer and the backbone show no clear trend. Only the azo experiences a higher effective temperature than the bulk temperature, with the spacer T_{eff} barely increasing to 42 °C and the backbone remaining at 40 °C. However, the effective temperature of the azo reaches only about 70 °C, approximately the bulk Tg, which is considerably lower than what was observed with the other wavelengths.

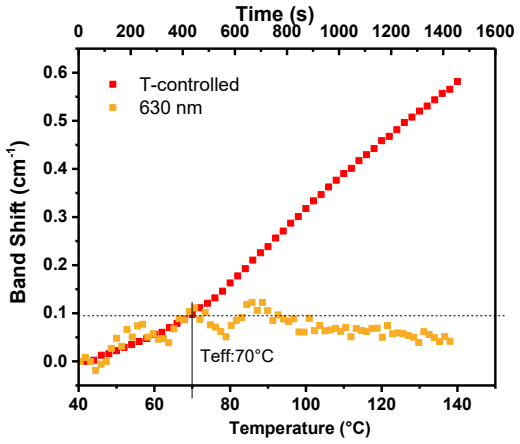

Figure 3.5: Band shift of the azo band (1335 cm^{-1}) under irradiation at 630 nm overlaid with the azo's band shift upon heating to determine the effective temperature.

Figure 3.4 also provides insight on the relaxation process of the molecule after irradiation. While the azo reaches a higher effective temperature than the spacer at all wavelengths studied, it also thermally relaxes faster and more completely towards its starting environment. While the spacer reaches a quasi-plateau after 2 min of thermal relaxation, the azo relaxes an additional 10-15 °C during the 12 min relaxation. This has previously been attributed to the slow movement of glassy matrixes below Tg.[6] As a consequence, there is a crossover point during relaxation at which the effective temperature of the azo becomes lower than the effective temperature of the spacer. The residual T_{eff} perturbation at the end of relaxation, shown in Table 3.2, is 26-57 % lower for the azo than it is for the spacer, again indicating that the azo relaxes more during the thermal relaxation than the spacer. In fact, the T_{eff} of the azo, which was well above Tg during irradiation, becomes lower than Tg after about 2 min of relaxation. In contrast, the T_{eff} of the spacer appears to remain stuck at a value close to the bulk Tg (71 °C) of gDR1. Despite reaching a similar T_{eff} under irradiation of 520 or 450 nm, the azo relaxes faster after the irradiation at 450 nm and arrives at an effective temperature 5 °C lower. Although the spacer reaches a higher effective temperature under 450 nm than 520 nm, it relaxes an additional 10 °C after 12 min with both wavelengths. The increase in T_{eff} as well as the relaxation process of the spacer is the same under 450 and 405 nm indicating that this segment of the molecule does not have the same wavelength dependence as the nitro group of the azo.

Further insight on the relaxation process is provided by applying the same biexponential fit to the thermal relaxation curves as was used to evaluate the cis content relaxation measured by UV-vis spectroscopy. Table 3.3 shows the fitting values obtained for the spacer and azo relaxation using Equation 3.2. The fit is not applied to the backbone since the band shift under irradiation does not increase enough to measure meaningful relaxation data. Having a y_0 value indicates a very long process associated with matrix relaxation. Fixing the value to zero would force the slow process to reach a band shift of zero at the end of the process, resulting in very long τ_2 values. The rate of the fast process is in the range of 17-24 s for the azo and 23-30 s for the spacer while the rate of the slow process is on the order of a few hundred seconds. During the fast process, cis isomers trapped in a stressed environment, where there is insufficient free volume in which they can move or provoke matrix plastic motion, relax rapidly in an elastic-like process.[59] The trans isomer resulting from this cis-trans conversion will thus be in an

environment similar to that before irradiation, that is with a bulk-like T_{eff}, and the overall effective temperature will decrease rapidly. The slow process, on the other hand, would account for the relaxation of azos in the amorphous regions with softer walls where the photoisomerization led to plastic-like deformation of the matrix.[59] In this case, the relaxation takes longer because the trans isomers are in a perturbed matrix environment where the effective temperature is higher and where the relaxation is slow because the bulk temperature is well below the Tg of the sample. In an orientation study, the fast process was attributed to the reversal of the angular hole burning process, where cis isomers return to the trans state, while the slow process was attributed to thermal rotational redistribution back to the isotropic state of the trans isomers that oriented perpendicular to the laser polarization by the angular redistribution process.[61] The weight is shifted onto A_1 for both the spacer and azo at all wavelengths. However, the spacer and azo have different values of A_1 and A_2 because they are in different parts of the molecule. The value of y_0 is smaller for the azo than the spacer, consistent with its lower T_{eff} values after relaxation. However, the difference between wavelengths for both groups is small. The ordering of y_0 versus wavelength for the spacer does however correspond to the trend observed in cis content.

Table 3.3: Thermal relaxation values obtained from fitting the band shift of selected bands following irradiation using Equation 3.2.

Wavelength, nm	**Spacer (C=O)**					**Azo (NO_2)**				
	y_0, cm^{-1}	A_1	τ_1, s	A_2	τ_2, s	y_0, cm^{-1}	A_1	τ_1, s	A_2	τ_2, s
520	0.6	0.5	30	0.3	389	0.05	0.3	21	0.1	262
	0.1	*0.1*	*5*	*0.1*	*115*	*0.04*	*0.05*	*2.5*	*0.01*	*51*
450	0.8	0.7	23	0.4	323	0.03	0.3	17	0.1	271
	0.1	*0.1*	*4*	*0.2*	*72*	*0.02*	*0.04*	*1*	*0.01*	*77*
405	0.6	0.5	26	0.6	664	0.03	0.2	24	0.1	302
	0.5	*0.1*	*4*	*0.3*	*534*	*0.00*	*0.02*	*1*	*0.00*	*69*
365	0.4	0.4	28	0.5	546	0.04	0.1	23	0.06	277
	0.04	*0.1*	*5*	*0.1*	*368*	*0.01*	*0.01*	*2*	*0.00*	*51*

Comparing the relaxation curves measured by infrared and UV-vis spectroscopy reveals that the effective temperature relaxation curve of the azo following 520 nm irradiation (Figure 3.4A) overlaps with the cis-content relaxation curve measured after irradiation at the same wavelength (Figure 3.1B). Consistently, the relaxation times for the UV-vis and IR spectroscopy (azo) results are very close in Tables 3.1 and 3.3 on the 12 min time scale. This suggests that the azo cis-trans relaxation, as probed by absorbance measurements, contributes to the relaxation of the local environment as probed by the IR spectroscopy band shift measurements for the azo moiety. A similar observation can be made for the relaxation curves after 450 nm irradiation. On the other hand, after 405 nm irradiation, the cis-content relaxation curve falls between the azo and spacer T_{eff} relaxation curves. Finally, after 365 nm irradiation, relaxation initially follows the curve of the spacer, but the slow process is slower. In all cases, after 12 min of relaxation, the effective temperature of the molecule has not reached its initial starting temperature. This implies that the matrix does not completely relax during the measurement time. The slow rate therefore accounts for the movement of the matrix below Tg.

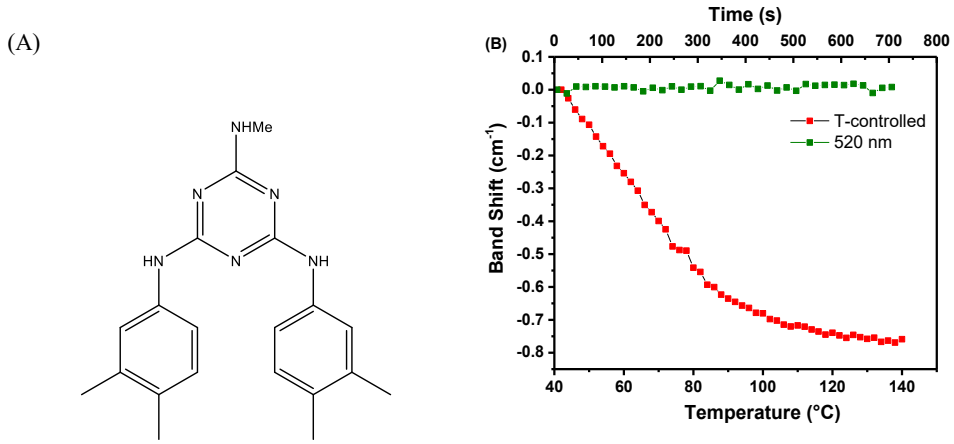

Figure 3.6: Molecular structure of g70 A) and band shift comparison under heating and irradiation at 520 nm for the triazine ring stretch of g70 (1563 cm^{-1}) B).

As a control experiment, the effects of cooling and irradiation were also measured on the molecular glass, g70, a compound that possess almost the same Tg as gDR1 (70 °C compared

to 71 °C) and shares a similar structure as gDR1 but without the presence of the azo moiety (see Figure 3.6 for structure). It is thus a good choice to ensure that optical heating is not responsible for the above observed effects under irradiation. As shown in Figure 3.6A, the band shift changes when heated but there is no change under irradiation and therefore no change in effective temperature felt. The results of irradiating g70 and gDR1 demonstrate that trans-cis-trans cycling of the azo moiety is essential for irradiation to provoke movement of the matrix.

3.3 Ellipsometry

Ellipsometry measurements under irradiation were taken to validate that photoexpansion occurs in thin films of gDR1 as was observed by Barrett et al.[29] in thin films of pDR1A. The thickness of the films was first measured prior to irradiation, and then during irradiation for 2 min followed by 12 min with the film in the dark (see Figure 3.7A). Figure 3.7B shows the normalized change in thickness of a gDR1 thin film under 2 min of irradiation at 520, 405 and 365 nm. The curves were normalized to reach the same thickness value in order to compare the growth of thickness under irradiation. These wavelengths were chosen because they are expected to produce different efficiencies of trans-cis-trans cycling. Photoexpansion of the film does indeed occur for gDR1 at all wavelengths studied. It saturates faster for 520 nm than it does for the other wavelengths, as shown by the curve in Figure 3.7B reaching a plateau. Irradiation for 15 min (not shown) with 520 and 405 nm light showed that the thickness did not continue to grow noticeably past what is overserved at two minutes, and therefore the irradiation time is sufficient for reaching saturation. On the other hand, it is clear from Figure 3.7B that saturation was not reached in 2 min for 365 nm irradiation, unlike the saturation reached at this wavelength when measuring the effective temperature. The distinct behaviours may be the consequence of the different length scales probed by the two techniques. The faster LED-on kinetics of 520 nm irradiation is consistent with the higher effective temperature felt by the azo at this wavelength. The change in thickness after 2 min was 6 % for 520 nm, 5 % for 405 nm and only 2 % for 365 nm. Under irradiation, the thickness of the film grows because trans-cis-trans cycling causes it to expand. Once the light is turned off, the film relaxes as shown by a very slow decrease in the thickness. It has previously been shown using pDR1A that the film thickness increase upon irradiation is not completely reversible.[29] Barrett et al. showed that,

after irradiation, the film thickness would only partially decrease but that when continuing with an irradiation cycle, the same thickness increase and relaxation would be observed for every cycle, like the pattern of our IR experiments presented here (Figure 3.4). In their work, the thickness could only be returned to its initial value by thermally erasing the photomechanical history of the sample. During 12 min of relaxation, 28 % of the film relaxes after 520 nm irradiation compared to 24 % of the film irradiated with 405 nm, and 20 % of the film irradiated with 365 nm. While the change in thickness during relaxation appears very small, the normalized 520 and 405 nm curves overlap well with the effective temperature relaxation curves of the spacer. Therefore, it is likely that the macroscopic thickness change observed by ellipsometry is dominated by the relaxation of the matrix, which as previously stated is slow below the bulk Tg, as is the relaxation of the local chemical environment around the spacer groups because they are not directly affected by photoisomerization of the azo group.

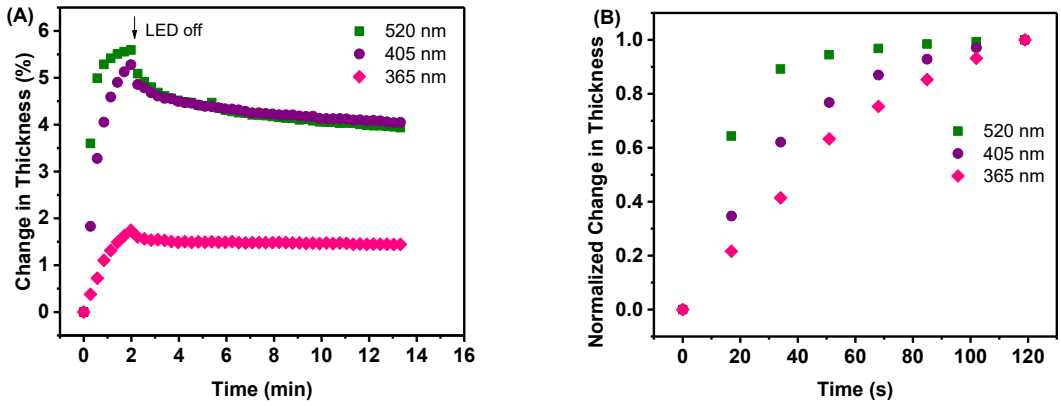

Figure 3.7: (A) Change in thickness of gDR1 upon irradiation and following thermal relaxation, and (B) normalized change in thickness of gDR1 under irradiation.

The change in thickness after irradiation was fitted using the same biexponential equation that was used with the UV-Vis and IR data (see Table 3.4). The time constants of the fast and slow processes are on the same order of magnitude as those measured by IR and UV-Vis spectroscopy. Comparing the weight of y_0 over the sum of y_0, A_1, and A_2 allows determining the relative percentage of relaxation that does not occur during the relaxation time related to the

fast and slow exponential relaxation processes (see Table 3.5). The weight of y_0 for the thickness yields values considerably higher than the equivalent values for cis content and effective temperature. The azo T_{eff} has the smallest weight. The cis content and T_{eff} of the spacer have the same weight when irradiated with 520 nm. The value is largest in all cases when irradiating with 365 nm. This calculation shows that upon 12 min of relaxation, the effective temperatures of the azo and spacer relax significantly despite the considerable fraction of cis isomers that have not relaxed and the very small relaxation of the film thickness. Given that the cis relaxation was only measured for 2 min, it should be expected that upon 12 min of relaxation, the weight of y_0 would be smaller.

Table 3.4: Thermal relaxation values of the thickness as measured by ellipsometry.

Wavelength, nm	**y_0**	**A_1**	**τ_1**	**A_2**	**τ_2**	**Thickness Change, %**	**% Relaxation**
520	1.0	0.2	22	0.2	354	6	28
	0.3	*0.03*	*12*	*0.1*	*47*	*1*	*7*
405	1.0	0.1	16	0.2	324	5	24
	0.2	*0.01*	*3*	*0.01*	*26*	*1*	*4*
365	1.5	0.1	8	0.3	222	2.0	20
	0.01	*0.05*	*4*	*0.01*	*25*	*0.5*	*8*

Table 3.5: Relative weight of y_0 obtained by measuring the cis content (2 min), effective temperature (12 min), and thickness (12 min) during thermal relaxation.

Method	**Cis Content**	**Effective temperature**		**Thickness**
Wavelength, nm		Spacer	Azo	
520	42	41	12	71
405	60	37	10	75
365	67	33	19	78

3.4 Differential Scanning Calorimetry

Annealing a molecular glass (or amorphous materials in general) below its Tg has the effect of allowing the material to structurally relax towards its ideal glass state. The ideal state is that of a glass with the same thermodynamics as extrapolated from the liquid state under

equilibrium. This causes the specific volume, and thus the free volume, to decrease. The effect of annealing can be quantified by measuring the enthalpy difference between the heating scans of an annealed and unannealed sample. The heating scan of an annealed sample will show a larger heat capacity peak upon going through the glass transition. Figure 3.8A shows representative heating scans of a sample of gDR1 with and without annealing, as well as the curve representing their difference that allows determining the enthalpic relaxation.

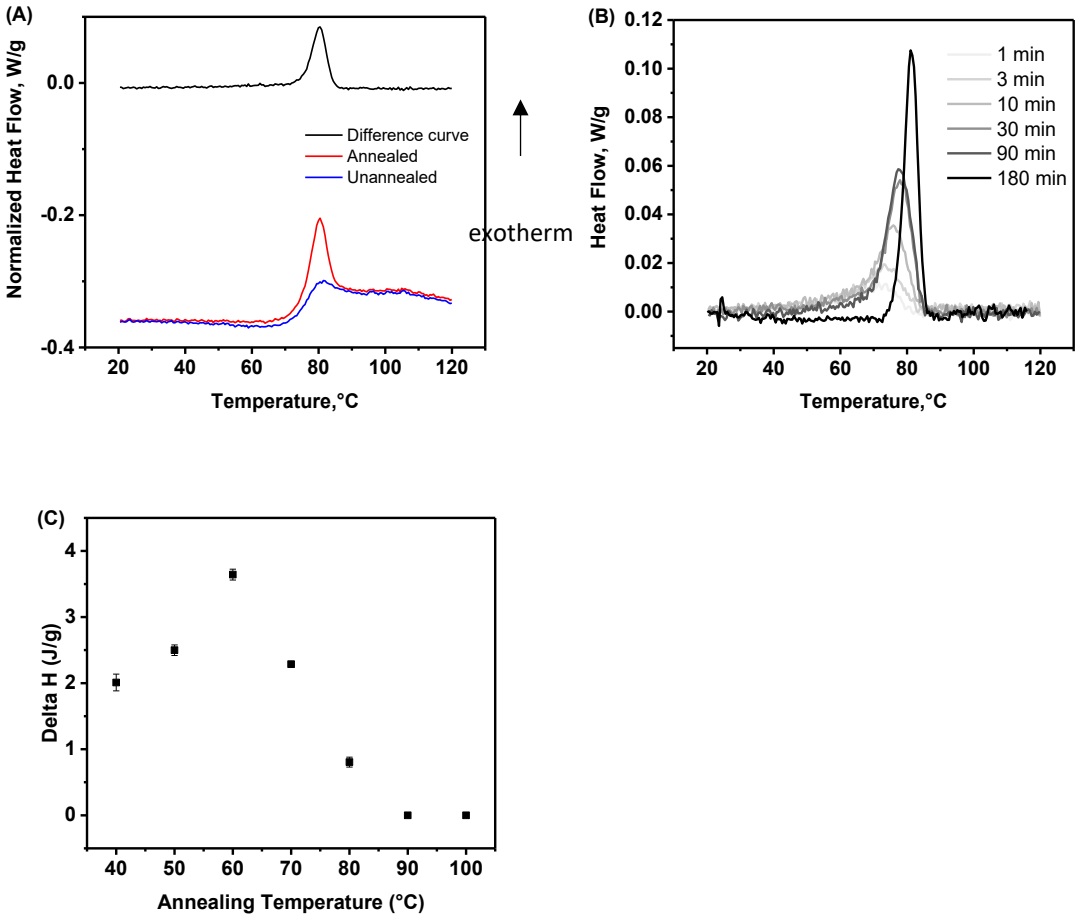

Figure 3.8: A) Heating scans for a sample of gDR1 with and without annealing and the resulting difference in heat flow between them, B) Difference heat flow curves of gDR1 annealed at 60 °C for various times, and C) enthalpy relaxation values measured after annealing gDR1 for 30 minutes at various temperatures.

The degree to which the material structurally relaxes is dependant on the annealing time and the annealing temperature. Figure 3.8B demonstrates that increasing the annealing time at

a fixed annealing temperature gradually increases ΔH (area of the peak) and shifts the peak to higher temperatures. This is due to the larger decrease in free volume during a longer relaxation. On the other hand, the temperature dependence of the enthalpy relaxation that is generated for a fixed annealing time follows a bell shape. As the temperature becomes further from Tg the annealing is less effective because the sample is either in the viscous state (above Tg) or the kinetics of structural relaxation become increasingly slower (below Tg). As shown in Figure 3.8C, there is an ideal temperature where the annealing is most effective. Figure 3.8C shows that for gDR1, annealing at Tg-11 produces the largest enthalpy value when comparing annealings of the same duration. This optimal annealing temperature decreases when increasing the constant annealing time.

Before acquiring the results of annealed gDR1 with and without irradiation, g70 (Tg of 70 °C) and pDR1A (Tg of 85 °C) were used as control samples to observe the expected behaviour of the material. As shown in Figure 3.6, g70 has the same triazine core as gDR1 and therefore shows the glass behaviour in the absence of the azo group. With pDR1A serving as the polymer counterpart of gDR1, and being a widely studied compound, it allows verifying that the experimental procedure followed is correct. As shown in Figure 3.9, the enthalpy relaxation measured for both samples increases with annealing time and temperature. It is interesting to note that annealing pDR1A for less than 10 minutes does not produce an enthalpy peak. Although the Tg is expected to tend towards the annealing temperature, no clear trend can be observed.

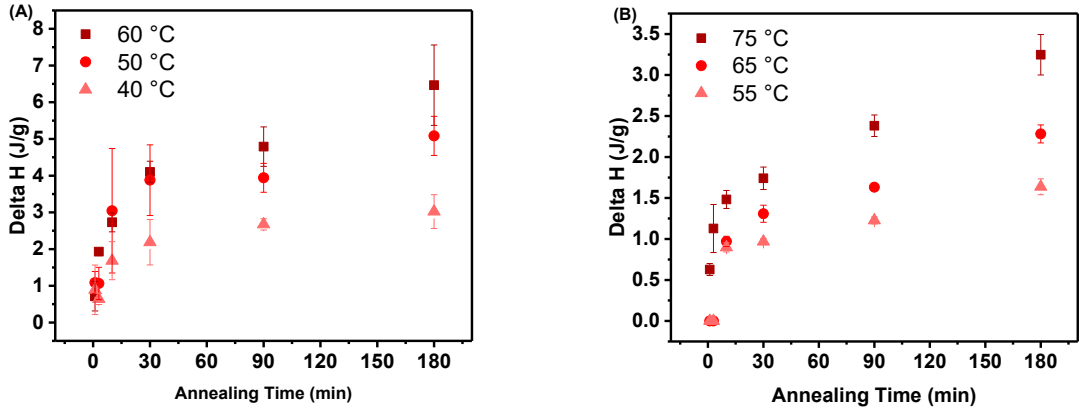

Figure 3.9: Enthalpy relaxation values measured upon annealing A) g70 and B) pDR1A at Tg-10, Tg-20 and Tg-30 °C for various times.

After confirming that the experimental procedure followed was appropriate, the annealing experiment was repeated with gDR1 using the same annealing times as the previous experiment at 40, 60 and 70 °C, the last chosen in order to observe the effect of annealing near Tg. As shown in Figure 3.10, the enthalpy increases with annealing time as expected. Like with g70, the enthalpy is larger when annealing at 60 °C than 40 °C. Annealing at 70 °C results in similar enthalpy changes to what is observed at 40 °C. This is evidence of the previously mentioned optimal annealing temperature. To determine if there is a limit on the enthalpy relaxation continuing to increase by prolonging the annealing time, annealing for 6 h at 40 °C is added to the curve. This point indicates the approach of a plateau where the enthalpy relaxation reaches a maximum as it does not increase within experimental uncertainty compared to 3 h of annealing. A detailed analysis of the thermograms did not reveal an observable trend in Tg or fictive temperature (Tf, the temperature at which the enthalpy of the glass would be equal to the enthalpy of the supercooled liquid under equilibrium).

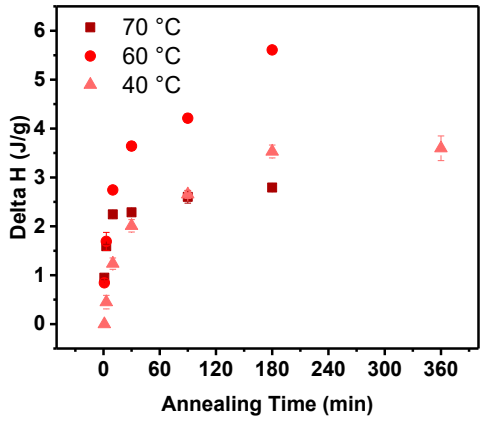

Figure 3.10: Enthalpy relaxation values measured upon annealing gDR1 at Tg-1, Tg-11 and Tg-31 °C for various times.

The experiment was then repeated with an added component of irradiation prior to measuring the heating scans to determine what effect irradiation has on the enthalpy relaxation. 520 and 405 nm are the chosen wavelengths of irradiation in order to see the effect of irradiation near the maximum of the trans absorbance with efficient trans-cis-trans cycling, and in the region weakly absorbed by both isomers and leading to less efficient cycling. Annealing temperatures of 60 and 40 °C are chosen annealing temperatures in order to observe the effect near the maximum of enthalpy relaxation as well as at the temperature used for the IR spectroscopy measurements of photoinduced changes in effective temperature. Figure 3.11A compares the difference heat flow curves for 360 and 90 min annealing at 40 °C with and without irradiation at 520 nm for 2 min. When the sample is irradiated, the enthalpy relaxation value measured is smaller. The peak of the curve is also shifted to higher temperatures compared to the corresponding curve without irradiation. Figure 3.11B shows that irradiation with 405 nm light also reduces the enthalpy relaxation. To confirm that 2 min of irradiation was long enough for the change in enthalpy to reach saturation, irradiation was also done for 15 min. Figure 3.11B shows that irradiation for 2 or 15 min with 405 nm light results in an enthalpy curve with similar peak area and therefore that 2 min are sufficient to reach a plateau. This is consistent with the observations made by IR spectroscopy and ellipsometry in terms of effective temperature and thickness change.

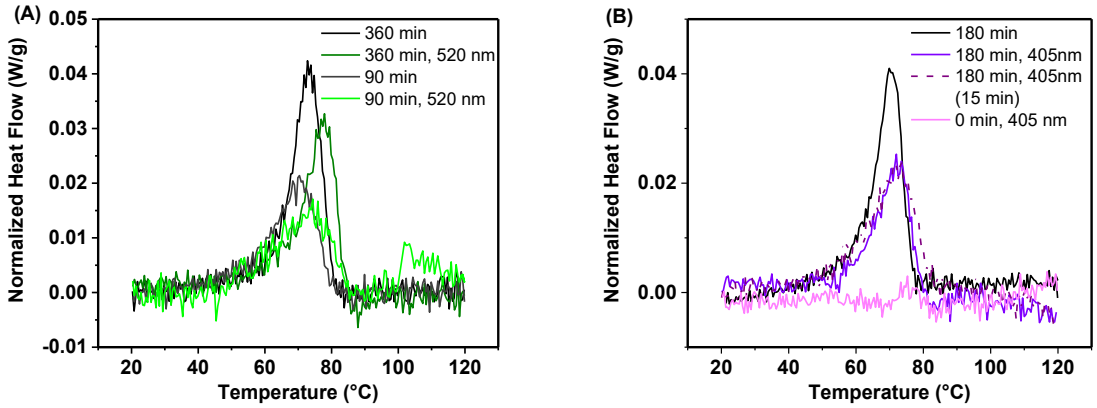

Figure 3.11: Enthalpy curves of gDR1 annealed at 40 °C under various conditions and partially erased with (A) 520 nm light, and (B) 405 nm light.

Figure 3.12 shows a plot of the enthalpy relaxation values measured after annealing gDR1 at 40 °C for various times without irradiation and with the same annealing followed by irradiation with 520 or 405 nm light. Irradiation of the annealed samples systematically decreases the value of ΔH for all annealing times. In other words, light has a rejuvenation effect on the sample and partially erases its thermal history. The maximal decrease in enthalpy relaxation is 1.2 J/g (refer to Figure 3.13 for 60 °C annealing). Light of 520 nm erases the enthalpy more than 405 nm light for all annealing times. This can be attributed to the stronger absorbance of the trans isomer at 520 nm leading to more cycling, a higher cis content and a larger increase in free volume. The changes in enthalpy associated with irradiation do not appear to depend on the annealing time, with the average enthalpy change at 40 °C after 520 nm irradiation being 1.0 ± 0.2 J/g, after 405 nm irradiation being 0.6 ± 0.3 J/g, and at 60 °C after 520 nm irradiation being 0.8 ± 0.2 J/g. This suggests that the annealing is not necessary for the irradiation to affect the increase in enthalpy of azomaterials (observed here indirectly as a light-induced reduction of the enthalpy relaxation). This was confirmed by irradiation of an unannealed sample which produced a negative enthalpy relaxation peak with 520 nm irradiation (see Figure 3.13A) as opposed to a very short annealing (1 min) where the enthalpy was completely erased (Figure 3.12). Nevertheless, the annealing of the sample before irradiation makes the determination of the effect of irradiation easier to measure as the relaxation peak is

better defined and less sensitive to baseline drift. In fact, irradiation with 405 nm has no quantifiable effect (see Figure 3.11B) on the unannealed sample while the photoinduced rejuvenation effect is clear when the sample is annealed first. There is no observable trend in the Tg measured by changing the conditions applied to the samples. However, the fictive temperature is generally smaller than the Tg for the same heating scan, and the Tg of the first heating scan measured is smaller than the second heating scan.

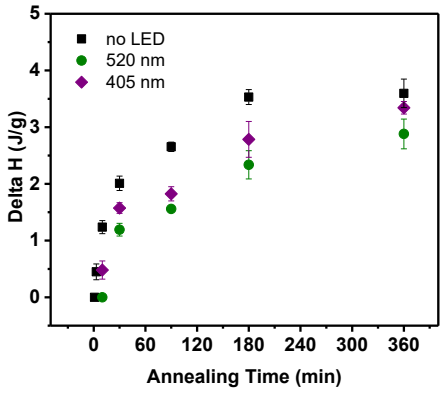

Figure 3.12: Enthalpy relaxation values measured for gDR1 annealed for various times at 40 °C without irradiation and followed by irradiation at 520 or 405 nm.

In addition to irradiating the sample after annealing, the irradiation can also be done prior to annealing to see if the enthalpy relaxation is also affected. As shown in Figure 3.13B, the enthalpy values measured show no clear difference when irradiating prior to annealing at 60 °C for both wavelengths. This lack of difference, contrary to our expectations, could be explained by the fast initial relaxation immediately after irradiation because of the higher free volume. The effect of irradiation is therefore lost faster and is not measurable when annealing the sample for several minutes. The same observation is made when annealing at 40 °C. Irradiating at 25 °C had a similar effect to irradiating at 40 °C. This was done as a control experiment to ensure that measurements taken at room temperature, for UV-vis and ellipsometry, can be compared to the DSC and ATR measurements conducted at 40 °C without the concern of temperature effects.

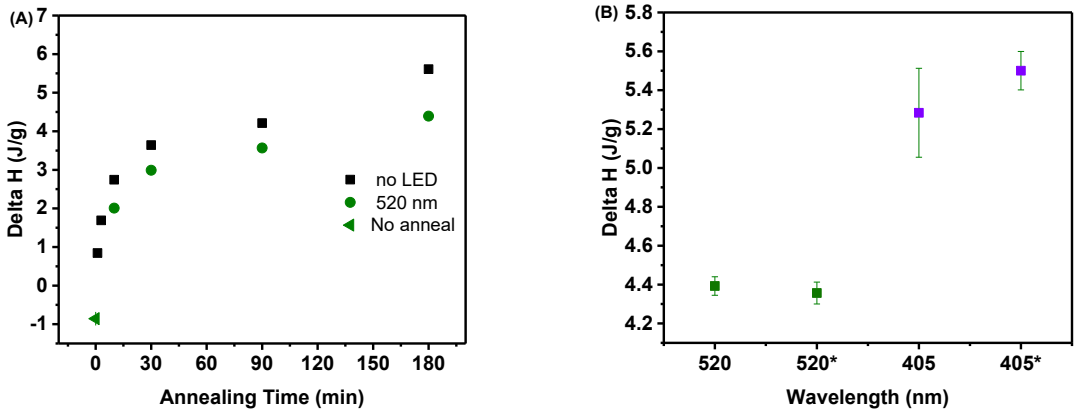

Figure 3.13: (A) Enthalpy relaxation values measured for gDR1 annealed at 60 °C and irradiated under different conditions and (B) annealed for 180 min at 60 °C (* indicates irradiation prior to annealing).

The observed enthalpy relaxation for irradiated samples is related to the amount of free volume generated during the irradiation. When a sample is irradiated, trans-cis-trans cycling generates additional free volume and increases the sample enthalpy, thereby partially erasing the structural relaxation that had occurred during annealing. The erasure of enthalpy relaxation is likely limited by the amount of free volume that can be created under irradiation. As previously shown, the backbone experiences only a very small increase in effective temperature compared to the spacer and azo moieties because free volume changes decrease with distance from the isomerizing unit. The azo moiety, however, shows a large photoinduced increase in effective temperature followed by fast relaxation. The smaller effect of 405 nm irradiation on the enthalpy is consistent with the smaller effective temperature reached by the azo at this wavelength. Despite having the same azo fraction, each azo undergoes fewer isomerization cycles, leading to a lower capability of affecting the matrix. The molecular weight composition of the material is approximately 38 % backbone, 23 % spacer, and 39 % azo. The percentage of the maximum decrease in enthalpy, 1.2 J/g, over the maximum enthalpy measured, 3.5 J/g at 40 °C, is 34 %. This value is similar to the molecular volume occupied by the azo moiety. Therefore, it is likely that the erasure of enthalpy corresponds to the azo group cycling, with the

remaining enthalpy relaxation after irradiation representative of the limit on the matrix movement.

Chapter 4

Conclusions and Future Work

4.1 Conclusions

The goal of this project was to determine if the phenomenon of photomobility in azobenzene-derived materials, which results in macroscopic photoinduced mass transport, can be attributed to light-stimulated structural relaxation. The project builds on work previously done by the group where the molecular environment of gDR1 and pDR1A under 520 nm irradiation was examined through IR spectroscopy. The previous work found that irradiation leads to heterogeneous changes in the molecules leading to the hypothesis that structural relaxation results in mass transport. Molecular glass gDR1 was selected for the project because it is derived from the widely studied DR1 chromophore, it undergoes rapid and repeated cis-trans-cis isomerization upon UV-visible irradiation and has previously shown to efficiently form surface relief gratings. Four wavelengths of light for irradiation were selected in order to examine the wavelength dependence of the molecular photomobility as well as the efficiency of trans-cis-trans isomerization. The wavelengths selected allow comparing the effect of irradiation near the absorbance maximum of the gDR1 trans isomer, its cis isomer, and in the region where both isomers absorb weakly. Four techniques were chosen to investigate photoinduced changes to the molecule at different length scales. UV-visible spectroscopy allowed measuring the isomer composition, infrared spectroscopy provided information on the chemical environment at the submolecular scale, ellipsometry allowed measuring the film thickness on a macroscopic scale and finally, differential scanning calorimetry allowed measuring enthalpic relaxation on the macroscopic scale.

In the first experiment, UV-visible spectroscopy was used to determine the minimum cis content in the photostationary state during irradiation. Upon irradiation the trans absorbance band decreased while the cis absorbance band increased due to trans-cis photoisomerization. The minimum cis content measured ranged from 7.7 to 13 %. Irradiation at 520 nm led to the most efficient absorption of the trans isomer, closely followed by 450 nm irradiation, which is consistent with their proximity to the absorbance maximum of the trans absorbance band. The

cis content measured is, however, close to that measured with 405 and 365 nm irradiation, where the absorbance of the trans isomer is considerably lower, because of the much higher efficiency of trans-cis-trans isomerization cycling at higher wavelengths. When the irradiation generated a higher cis content with efficient cycling, and therefore generated a higher free volume, cis relaxation was faster because there was more room for it to occur. The relaxation measured also showed the two-part process expected for push-pull type azo materials resulting from the inhomogeneous distribution of free volume inside the matrix. Cis isomers trapped in a strained environment with less free volume relax first in a fast process, followed by a slow process where cis isomers relax in a non-stressed environment with a large fraction of free volume.

Next, IR spectroscopy was used to measure the local temperature, termed effective temperature, felt by the backbone, spacer and azo group of gDR1 under irradiation. At all wavelengths, the effective temperature of the azo was highest, followed by the spacer, while only a small increase was detected for the backbone. This is a result of the decrease in local free volume with distance from the isomerizing azo group. For the azo group, wavelengths associated with more efficient cycling led to higher effective temperatures indicating a wavelength dependence. On the other hand, the spacer group did not show the same dependence as its local environment was the same under 450 and 405 nm irradiation. The azo demonstrated a faster thermal relaxation than the spacer in all cases. The different effective temperatures felt along the molecule are confirmation of the fluid-like properties felt by the azo moiety under irradiation when the bulk temperature of the sample would put the molecule in the glassy state.

Photoexpansion of gDR1 films was then measured through ellipsometry. Photoexpansion of the film is a result of the generation of excess free volume in the sample due to trans-cis-trans cycling. Irradiation with 520 nm resulted in a change in thickness that saturates faster than with 405 and 365 nm irradiation. However, the change in thickness resulting from and following irradiation with 520 and 405 nm is very similar, while that of 365 nm is considerably smaller. The thickness relaxation curves after irradiation with 520 and 405 nm overlap with the effective temperature relaxation curves of the spacer after irradiation with the same wavelengths, indicating that the change in thickness is dominated by the relaxation of the matrix. A comparison of the kinetics measured with the three experiments revealed that while there is considerable relaxation of the effective temperature of the spacer and azo during the

time scale of measurement, there remains a significant fraction of isomers trapped in a perturbed matrix, that was provoked by the irradiation.

Finally, differential scanning calorimetry was used to measure the change in enthalpy relaxation that occurs during photoisomerization. First, samples of gDR1 were annealed for various times and at various temperatures. When annealed, the molecular glass structurally relaxes towards its ideal glass state, and the free volume decreases. The decrease in free volume was quantified indirectly by measuring the enthalpy changes. After annealing, the samples were irradiated in order to measure the amount of enthalpy relaxation that could be erased through trans-cis-trans cycling. A maximal decrease in enthalpy relaxation was measured to be 1.2 J/g, and a lack of trend with annealing time suggested that annealing prior to irradiation is not necessary for the irradiation to increase the enthalpy of the system. Irradiation with 520 nm led to a greater decrease in enthalpy relaxation than 405 nm because the wavelength produces more efficient cycling and therefore generates a greater free volume to counteract the effect of annealing. Irradiation for 15 min showed that saturation is reached upon 2 min of irradiation and therefore it is likely that the decrease in the measured enthalpy relaxation is limited by the amount of free volume that can be generated upon irradiation. Since the azo moiety shows the greatest increase in effective temperature and fastest relaxation, while the spacer and backbone relax more slowly, it is possible that the erasure of enthalpy corresponds to cycling of the azo group. The remaining enthalpy relaxation after irradiation would then be attributable to the limit on the matrix movement, which occurs on a longer time scale. Given the observed changes to the isomer populations, local environment and thickness of the film, and the measured kinetics of relaxation, it is reasonable to conclude that photomobility occurs as a result of light-stimulated enthalpic relaxation.

4.2 Future Work

The first continuation of this project is to complete the measurements taken with pDR1A to verify if a polymer with the same azo group behaves in the same way as the molecular glass. It will then be possible to compare the behaviour of both materials under irradiation, as measured through the different techniques. It can then be established if light-stimulated enthalpic relaxation is also the mechanism through which photomobility of the polymer occurs.

Additional DSC measurements could be taken with gDR1 in order to see the effect of shorter irradiation on the enthalpy. Since 2 min of irradiation showed evidence of a plateau, irradiating for shorter times would allow determining the minimum amount of irradiation required to provoke a change in the material. The results could then be compared to the "on" kinetics measured for the spacer through the effective temperature demonstrating the effect on the matrix. Further measurements under 630 nm irradiation could also be taken. The effective temperature continues to increase during the second and third cycle of irradiation suggesting the possibility of forming surface relief gratings with this wavelength. An additional experiment would be to take AFM images of the films used for ellipsometry to observe the smaller change in thickness measured after irradiation with 365 nm. This would provide insight on the distribution of the photoexpansion of the film by showing if there is a uniform or localised change in thickness in the film, in particular at the edges of the sample.

Similar experiments to those done in this project could then be done using an azo glass of the azobenzene (ABn) type under irradiation conditions selected to generate a similar cis content to gDR1. This would result in the cis lifetime being much longer than that of the push-pull glass used here. It would then be possible to study the impact of generating a mostly cis state on the effective temperature and the erasure of enthalpic relaxation. The experiments could then be repeated with mixtures of photoactive and photopassive molecules as was previously done by the group in relation to surface relief gratings.[22] This would indicate the percentage of photoactive molecules needed in the mixture to generate photoinduced structural relaxation.

References

1. Hartley, G. S., The Cis-Form of Azobenzene. *Nature* **1937,** *140* (3537), 281-281.

2. Henzl, J.; Mehlhorn, M.; Gawronski, H.; Rieder, K. H.; Morgenstern, K., Reversible Cis-Trans Isomerization of a Single Azobenzene Molecule. *Angewandte Chemie Internal Edition English* **2006,** *45* (4), 603-606.

3. Bandara, H. M.; Burdette, S. C., Photoisomerization in Different Classes of Azobenzene. *Chemical Society Reviews* **2012,** *41* (5), 1809-1825.

4. Dong, M.; Babalhavaeji, A.; Samanta, S.; Beharry, A. A.; Woolley, G. A., Red-Shifting Azobenzene Photoswitches for in Vivo Use. *Accounts of Chemical Research* **2015,** *48* (10), 2662-2670.

5. Bahrenburg, J.; Rottger, K.; Siewertsen, R.; Renth, F.; Temps, F., Sequential Photoisomerisation Dynamics of the Push-Pull Azobenzene Disperse Red 1. *Photochemical & Photobiological Sciences* **2012,** *11* (7), 1210-1219.

6. Vapaavuori, J.; Laventure, A.; Bazuin, C. G.; Lebel, O.; Pellerin, C., Submolecular Plasticization Induced by Photons in Azobenzene Materials. *Journal of the American Chemical Society* **2015,** *137* (42), 13510-13517.

7. Rau, H., *Photoisomerization of Azobenzenes*. Elsevier Inc.: 2002; p 559.

8. Barrett, C.; Natansohn, A.; Rochon, P., Cis-Trans Thermal-Isomerization Rates of Bound and Doped Azobenzenes in a Series of Polymers. *Chemistry of Materials* **1995,** *7* (5), 899-903.

9. Baroncini, M.; Ragazzon, G.; Silvi, S.; Venturi, M.; Credi, A., The Eternal Youth of Azobenzene: New Photoactive Molecular and Supramolecular Devices. *Pure and Applied Chemistry* **2015,** *87* (6), 537-545.

10. Barrett, C. J.; Natansohn, A. L.; Rochon, P. L., Mechanism of Optically Inscribed High-Efficiency Diffraction Gratings in Azo Polymer Films. *Journal of Physical Chemistry* **1996,** *100* (21), 8836-8842.

11. Singleton, T. A.; Ramsay, K. S.; Barsan, M. M.; Butler, I. S.; Barrett, C. J., Azobenzene Photoisomerization under High External Pressures: Testing the Strength of a Light-Activated Molecular Muscle. *Journal of Physical Chemistry B* **2012,** *116* (32), 9860-9865.

12. Vetrakova, L.; Ladanyi, V.; Al Anshori, J.; Dvorak, P.; Wirz, J.; Heger, D., The Absorption Spectrum of Cis-Azobenzene. *Photochemical and Photobiolical Sciences* **2017,** *16* (12), 1749-1756.

13. Curtin, D. Y.; Grubbs, E. J.; McCarty, C. G., Uncatalyzed Syn-Anti Isomerization of Imines, Ozime Ethers, and Haloimines. *Journal of the American Chemical Society* **1966,** *88* (12), 2775-2786.

14. Kim, Y.; Phillips, J. A.; Liu, H.; Kang, H.; Tan, W., Using Photons to Manipulate Enzyme Inhibition by an Azobenzene-Modified Nucleic Acid Probe. *Proceedings of the National Academy of Sciences USA* **2009,** *106* (16), 6489-64894.

15. Muraoka, T.; Kinbara, K.; Aida, T., Mechanical Twisting of a Guest by a Photoresponsive Host. *Nature* **2006,** *440* (7083), 512-515.

16. Ikeda, T.; Sasaki, T.; Ichimura, K., Photochemical Switching of Polarization in Ferroelectric Liquid-Crystal Films. *Nature* **1993,** *361* (6411), 428-430.

17. Iwamoto, M.; Majima, Y.; Naruse, H.; Noguchi, T.; Fuwa, H., Generation of Maxwell Displacement Current across an Azobenzene Monolayer by Photoisomerization. *Nature* **1991,** *353* (6345), 645-647.

18. Yu, Y.; Nakano, M.; Ikeda, T., Photomechanics: Directed Bending of a Polymer Film by Light. *Nature* **2003,** *425* (6954), 145.

19. Kawano, K.; Ishii, T.; Minabe, J.; Niitsu, T.; Nishikata, Y.; Baba, K., Holographic Recording and Retrieval of Polarized Light by Use of Polyester Containing Cyanoazobenzene Units in the Side Chain. *Optics Letters* **1999,** *24* (18), 1269-1271.

20. Yesodha, S. K.; Pillai, C. K. S.; Tsutsumi, N., Stable Polymeric Materials for Nonlinear Optics: A Review Based on Azobenzene Systems. *Progress in Polymer Science* **2004,** *29* (1), 45-74.

21. Zakerhamidi, M. S.; Keshavarz, M.; Tajalli, H.; Ghanadzadeh, A.; Ahmadi, S.; Moghadam, M.; Hosseini, S. H.; Hooshangi, V., Isotropic and Anisotropic Environment Effects on the Uv/Vis Absorption Spectra of Three Disperse Azo Dyes. *Journal of Molecular Liquids* **2010,** *154* (2-3), 94-101.

22. Laventure, A.; Bourotte, J.; Vapaavuori, J.; Karperien, L.; Sabat, R. G.; Lebel, O.; Pellerin, C., Photoactive/Passive Molecular Glass Blends: An Efficient Strategy to Optimize

Azomaterials for Surface Relief Grating Inscription. *ACS Applied Material Interfaces* **2017,** *9* (1), 798-808.

23. Bennani, O. R.; Al-Hujran, T. A.; Nunzi, J. M.; Sabat, R. G.; Lebel, O., Surface Relief Grating Growth in Thin Films of Mexylaminotriazine-Functionalized Glass-Forming Azobenzene Derivatives. *New Journal of Chemistry* **2015,** *39* (12), 9162-9170.

24. Vapaavuori, J.; Heikkinen, I. T. S.; Dichiarante, V.; Resnati, G.; Metrangolo, P.; Sabat, R. G.; Bazuin, C. G.; Priimagi, A.; Pellerin, C., Photomechanical Energy Transfer to Photopassive Polymers through Hydrogen and Halogen Bonds. *Macromolecules* **2015,** *48* (20), 7535-7542.

25. Naito, T.; Horie, K.; Mita, I., Photochemistry in Polymer Solids. 11. The Effects of the Size of Reaction Groups and the Mode of Photoisomerization on Photochromic Reactions in Polycarbonate Film. *Macromolecules* **1991,** *24* (10), 2907-2911.

26. Ho, M. S.; Natansohn, A.; Rochon, P., Azo Polymers for Reversible Optical Storage .7. The Effect of the Size of the Photochromic Groups. *Macromolecules* **1995,** *28* (18), 6124-6127.

27. Chien, F. S. S.; Lin, C. Y.; Hsu, C. C., Local Photo-Assisted Poling of Azo Copolymer Films by Scanning Probe Microscopy. *Journal of Physics D-Applied Physics* **2008,** *41* (23), 235502-235508.

28. Vapaavuori, J.; Valtavirta, V.; Alasaarela, T.; Mamiya, J. I.; Priimagi, A.; Shishido, A.; Kaivola, M., Efficient Surface Structuring and Photoalignment of Supramolecular Polymer-Azobenzene Complexes through Rational Chromophore Design. *Journal of Materials Chemistry* **2011,** *21* (39), 15437-15441.

29. Tanchak, O. M.; Barrett, C. J., Light-Induced Reversible Volume Changes in Thin Films of Azo Polymers: The Photomechanical Effect. *Macromolecules* **2005,** *38* (25), 10566-10570.

30. Ando, H.; Tanino, T.; Nakano, H.; Shirota, Y., Photoinduced Surface Relief Grating Formation Using New Polymers Containing the Same Azobenzene Chromophore as a Photochoromic Amorphous Molecular Material. *Materials Chemistry and Physics* **2009,** *113* (1), 376-381.

31. Grebenkin, S.; Meshalkin, A. B., Wavelength Dependence of the Reorientation Efficiency of Azo Dyes in Polymer Matrixes. *Journal of Physical Chemistry B* **2017,** *121* (35), 8377-8384.

32. Rahmouni, A.; Bougdid, Y.; Moujdi, S.; Nesterenko, D. V.; Sekkat, Z., Photoassisted Holography in Azo Dye Doped Polymer Films. *Journal of Physical Chemistry B* **2016,** *120* (43), 11317-11322.

33. Rianna, C.; Calabuig, A.; Ventre, M.; Cavalli, S.; Pagliarulo, V.; Grilli, S.; Ferraro, P.; Netti, P. A., Reversible Holographic Patterns on Azopolymers for Guiding Cell Adhesion and Orientation. *ACS Applied Material Interfaces* **2015,** *7* (31), 16984-16991.

34. Kirby, R.; Sabat, R. G.; Nunzi, J. M.; Lebel, O., Disperse and Disordered: A Mexylaminotriazine-Substituted Azobenzene Derivative with Superior Glass and Surface Relief Grating Formation. *Journal of Materials Chemistry C* **2014,** *2* (5), 841-847.

35. Ediger, M. D.; Angell, C. A.; Nagel, S. R., Supercooled Liquids and Glasses. *Journal of Physical Chemistry* **1996,** *100* (31), 13200-13212.

36. Shirota, Y., Photo- and Electroactive Amorphous Molecular Materials - Molecular Design, Syntheses, Reactions, Properties, and Applications. *Journal of Materials Chemistry* **2005,** *15* (1), 75-93.

37. Laventure, A.; Soldera, A.; Pellerin, C.; Lebel, O., Heads Vs. Tails: A Double-Sided Study of the Influence of Substituents on the Glass-Forming Ability and Stability of Aminotriazine Molecular Glasses. *New Journal of Chemistry* **2013,** *37* (12), 3881-3889.

38. Shirota, Y., Organic Materials for Electronic and Optoelectronic Devices. *Journal of Materials Chemistry* **2000,** *10* (1), 1-25.

39. Wang, R. Y.; Pellerin, C.; Lebel, O., Role of Hydrogen Bonding in the Formation of Glasses by Small Molecules: A Triazine Case Study. *Journal of Materials Chemistry* **2009,** *19* (18), 2747-2753.

40. Tanino, T.; Yoshikawa, S.; Ujike, T.; Nagahama, D.; Moriwaki, K.; Takahashi, T.; Kotani, Y.; Nakano, H.; Shirota, Y., Creation of Azobenzene-Based Photochromic Amorphous Molecular Materials—Synthesis, Glass-Forming Properties, and Photochromic Response. *Journal of Materials Chemistry* **2007,** *17* (47), 4953-4963.

41. Narisawa, Y.; Komatsu, K.; Sugihara, O.; Tanino, T.; Nakano, H.; Shirota, Y.; Kaino, T., Fabrication and Evaluation of All-Optical 1x2 Y-Branch Waveguide Switch Using

Photochromic Amorphous Molecular Materials. *Integrated Optoelectronic Devices 2008* **2008,** *6891*.

42. Nakano, H.; Takahashi, T.; Tanino, T.; Shirota, Y., Synthesis and Photoinduced Surface Relief Grating Formation of Novel Photo-Responsive Amorphous Molecular Materials, 4-[Bis(9,9-Dimethylfluoren-2-Yl)Amino]-4′-Cyanoazobenzene and 4-[Bis(9,9-Dimethylfluoren-2-Yl)-Amino]-4′-Nitroazobenzene. *Dyes and Pigments* **2010,** *84* (1), 102-107.

43. Snell, K. E.; Hou, R.; Ishow, E.; Lagugne-Labarthet, F., Enhanced Rates of Photoinduced Molecular Orientation in a Series of Molecular Glassy Thin Films. *Langmuir* **2015,** *31* (26), 7296-7305.

44. Nakano, H.; Ichikawa, R.; Ukai, H.; Kitano, A., Photoinduced Shape Changes of Mixed Molecular Glass Particles Containing Azobenzene-Based Photochromic Amorphous Molecular Materials Fixed in Agar Gel. *Journal of Physical Chemistry B* **2018,** *122* (31), 7775-7781.

45. Nakano, H.; Tanino, T.; Takahashi, T.; Ando, H.; Shirota, Y., Relationship between Molecular Structure and Photoinduced Surface Relief Grating Formation Using Azobenzene-Based Photochromic Amorphous Molecular Materials. *Journal of Materials Chemistry* **2008,** *18* (2), 242-246.

46. Laventure, A.; De Grandpre, G.; Soldera, A.; Lebel, O.; Pellerin, C., Unraveling the Interplay between Hydrogen Bonding and Rotational Energy Barrier to Fine-Tune the Properties of Triazine Molecular Glasses. *Physical Chemistry Chemical Physics* **2016,** *18* (3), 1681-1692.

47. Lebel, O.; Maris, T.; Perron, M. E.; Demers, E.; Wuest, J. D., The Dark Side of Crystal Engineering: Creating Glasses from Small Symmetric Molecules That Form Multiple Hydrogen Bonds. *Journal of the American Chemical Society* **2006,** *128* (32), 10372-10373.

48. Lefin, P.; Fiorini, C.; Nunzi, J. M., Anisotropy of the Photo-Induced Translation Diffusion of Azobenzene Dyes in Polymer Matrices. *Pure and Applied Optics* **1998,** *7* (1), 71-82.

49. Teboul, V.; Saiddine, M.; Nunzi, J. M.; Accary, J. B., An Isomerization-Induced Cage-Breaking Process in a Molecular Glass Former Below T(G). *Journal of Physical Chemistry* **2011,** *134* (11), 114517.

50. Saphiannikova, M.; Toshchevikov, V., Optical Deformations of Azobenzene Polymers: Orientation Approach Vs. Photofluidization Concept. *Journal of the Society for Information Display* **2015,** *23* (4), 146-153.

51. Harrison, J. M.; Goldbaum, D.; Corkery, T. C.; Barrett, C. J.; Chromik, R. R., Nanoindentation Studies to Separate Thermal and Optical Effects in Photo-Softening of Azo Polymers. *Journal of Materials Chemistry C* **2015,** *3* (5), 995-1003.

52. Karageorgiev, P.; Neher, D.; Schulz, B.; Stiller, B.; Pietsch, U.; Giersig, M.; Brehmer, L., From Anisotropic Photo-Fluidity Towards Nanomanipulation in the Optical near-Field. *Nature Materials* **2005,** *4* (9), 699-703.

53. Ishitobi, H.; Tanabe, M.; Sekkat, Z.; Kawata, S., The Anisotropic Nanomovement of Azo-Polymers. *Optics Express* **2007,** *15* (2), 652-659.

54. Richter, A. N., M.; Wolf, B. , A Nanoidentation Study of Photo-Induced Changes in Polymers Containing Azobenzene. *Molecular Crystals and Liquid Crystals* **2008,** *483*, 49-61.

55. Vapaavuori, J.; Mahimwalla, Z.; Chromik, R. R.; Kaivola, M.; Priimagi, A.; Barrett, C. J., Nanoindentation Study of Light-Induced Softening of Supramolecular and Covalently Functionalized Azo Polymers. *Journal of Materials Chemistry C* **2013,** *1* (16), 2806-2810.

56. Fang, G. J.; Maclennan, J. E.; Yi, Y.; Glaser, M. A.; Farrow, M.; Korblova, E.; Walba, D. M.; Furtak, T. E.; Clark, N. A., Athermal Photofluidization of Glasses. *Nature Communications* **2013,** *4*, 1521-1531.

57. Coelho, P. J.; Sousa, C. M.; Castro, M. C. R.; Fonseca, A. M. C.; Raposo, M. M. M., Fast Thermal Cis–Trans Isomerization of Heterocyclic Azo Dyes in PMMA Polymers. *Optical Materials* **2013,** *35* (6), 1167-1172.

58. Airinei, A.; Fifere, N.; Homocianu, M.; Gaina, C.; Gaina, V.; Simionescu, B. C., Optical Properties of Some New Azo Photoisomerizable Bismaleimide Derivatives. *International Journal of Molecular Sciences* **2011,** *12* (9), 6176-6193.

59. Wang, C.; Weiss, R. G., Thermal Cis → Trans Isomerization of Covalently Attached Azobenzene Groups in Undrawn and Drawn Polyethylene Films. Characterization and Comparisons of Occupied Sites. *Macromolecules* **2003,** *36* (11), 3833-3840.

60. Tabone, R.; Barra, M., Thermal Cis-to-Trans Isomerisation of Triazene Dyes in Doped Polymer Films. *Dyes and Pigments* **2011,** *88* (2), 180-186.

61. Wang, X. X.; Vapaavuori, J.; Bazuin, C. G.; Pellerin, C., Molecular-Level Study of Photoorientation in Hydrogen-Bonded Azopolymer Complexes. *Macromolecules* **2018,** *51* (3), 1077-1087.